



Cite this: *Environ. Sci.: Adv.*, 2026, 5, 997

## Recent advances in biochar-based engineered materials for efficient removal of CO<sub>2</sub>: from lab to industrial scale applications

Anass Wahby,<sup>a</sup> Nouha El Mail,<sup>a</sup> Youssef Aoulad El Hadj Ali,<sup>a</sup> Abdelmonaim Azzouz,<sup>\*a</sup> Brahim Arhoun,<sup>a</sup> Mounir Manssouri,<sup>b</sup> Mostafa Stitou<sup>a</sup> and Suresh Kumar Kailasa<sup>\*c</sup>

Growing concerns about greenhouse gas emissions have driven significant efforts toward developing advanced materials for the capture and removal of carbon dioxide (CO<sub>2</sub>) from different environments. Among these, biochar-based engineered materials have emerged as promising sorbents for physical adsorption and separation processes, owing to their tunable structure, surface functionality, and potential for scalable production. This review summarizes recent advances in the preparation and application of biochar-based engineered materials for CO<sub>2</sub> capture, highlighting the influence of synthesis methods on their structural properties and adsorption performance. A comparative analysis of different biochar-derived materials is presented, focusing on adsorption capacity, selectivity, and reusability. Notably, woody biomass-derived biochar modified with vanadium oxide demonstrated exceptional performance, achieving a CO<sub>2</sub> adsorption capacity of 9.8 mmol g<sup>-1</sup> and maintaining stability over 11 adsorption–desorption cycles with minimal loss of efficiency. The review also discusses the key challenges that currently limit large-scale deployment of biochar-based adsorbents and proposes potential strategies to overcome these barriers, thereby outlining future research directions toward sustainable and efficient CO<sub>2</sub> capture technologies.

Received 21st November 2025  
Accepted 18th February 2026

DOI: 10.1039/d5va00432b

rsc.li/esadvances

### Environmental significance

In recent years, CO<sub>2</sub> levels have exceeded 400 ppm globally, causing the greenhouse effect. As a result, capturing of CO<sub>2</sub> plays a key role in minimizing the greenhouse effect. In view of this, surface engineered biochar has been used as a potential adsorbent for the capturing and removal of CO<sub>2</sub> from various environments. The selectivity of biochar is greatly enhanced by activating its surface with different functional groups and nanostructures, thereby improving its adsorption capacity toward CO<sub>2</sub>. Engineered biochar materials have demonstrated strong potential for capturing CO<sub>2</sub> from various environments and converting it into value-added products, thereby contributing to the mitigation of the greenhouse effect.

## 1 Introduction

Global warming, driven by greenhouse gas emissions, is one of the most pressing environmental challenges worldwide that require immediate action. Among the many greenhouse gases (e.g., CO<sub>2</sub>, CH<sub>4</sub> and N<sub>2</sub>O), carbon dioxide (CO<sub>2</sub>) is the most significant contributor.<sup>1</sup> Recent reports revealed that the levels of global CO<sub>2</sub> have exceeded 400 ppm.<sup>2</sup> Moreover, the reports of the Intergovernmental Panel on Climate Change (IPCC) demonstrated that the concentration of global CO<sub>2</sub> is expected

to reach 950 ppm by 2100, causing serious environmental issues such as glacial melting, ocean acidification, and extreme weather.<sup>3</sup> Therefore, efficient CO<sub>2</sub> capture and sequestration technologies are essential to reduce atmospheric CO<sub>2</sub> emissions, thereby protecting the environment and stabilizing the climate system.

Currently, the primary approaches to eliminate CO<sub>2</sub> from the atmosphere include membrane separation, absorption, adsorption, cryogenic separation, hydrate and chemical looping combustion, and so on.<sup>4</sup> Adsorption is extensively used in the elimination of CO<sub>2</sub> due to its low energy requirement, low cost of adsorbent materials, adsorbent material regeneration, easy implementation, high efficiency, cost-effective process technology, and high CO<sub>2</sub> uptake capacity.<sup>5</sup> In view of this, several carbon-based materials such as biochar, carbon nanotubes (CNTs), multi-walled carbon nanotubes (MWCNTs), single-walled carbon nanotubes (SWCNTs), microporous carbon,

<sup>a</sup>Laboratory of Water, Research, and Environmental Analysis, Faculty of Sciences, Abdelmalek Essaadi University, Tetouan, Morocco. E-mail: aazzouz@uae.ac.ma

<sup>b</sup>Research Team on Natural Products Chemistry and Smart Technologies (NPC-ST), Polydisciplinary Faculty of Larache, Abdelmalek Essaadi University, Tetouan, Larache, Morocco

<sup>c</sup>Department of Chemistry, Sardar Vallabhbhai National Institute of Technology, Surat-395 007, Gujarat, India. E-mail: skk@chem.svmit.ac.in



graphene, graphene oxide (GO), reduced graphene oxide (rGO), carbon dots (CDs), and graphene/carbon quantum dots (G/CQDs) have proven to be highly efficient and promising materials in adsorbing and capturing CO<sub>2</sub> from the atmosphere.<sup>6,7</sup> However, expensive synthetic tools are required for the fabrication of carbon nanomaterials (CNTs, graphene, and activated carbon), limiting their wider applications in CO<sub>2</sub> removal.<sup>8</sup> Biochar, a porous carbon-based substance made generally from organic waste, is widely used as a potential sorbent in capturing CO<sub>2</sub> due to its several advantages such as simplicity, low cost and eco-friendly nature.<sup>9</sup> In addition, greenhouse gases are effectively adsorbed by biochar due to its structural features.<sup>10</sup> To support this, biochar-based engineered materials were successfully used as potential adsorbents for capturing CO<sub>2</sub>, ranging from 1 to 35 gigatons (GtCO<sub>2</sub>) and 78 to 477 GtCO<sub>2</sub>.<sup>10</sup> In the last few years, studies on CO<sub>2</sub> adsorption onto biochar have increased. Fig. 1 represents the data obtained in Scopus by searching the keywords “carbon dioxide” and “biochar”, suggesting that significant efforts have been made on the use of biochar-based materials for the removal of CO<sub>2</sub> from industrial and environmental sources.

Numerous synthetic methodologies such as hydrothermal carbonization, pyrolysis, gasification and torrefaction were utilized for the preparation of biochar engineered materials from various chiefly available biomass feedstocks and wastes as carbon sources (dairy manure, forestry, agricultural, and other solid bio-wastes).<sup>8,11,12</sup> Although the biochar materials produced were successfully applied for the removal of CO<sub>2</sub>, unfortunately they exhibited certain shortcomings of pristine biochar (narrow adsorption ranges, low adsorption capacity and other limitations), which limit their wide applications in removing CO<sub>2</sub>. Consequently, the strategic modification or “engineering” of biochar to enhance its CO<sub>2</sub> adsorption properties has emerged as a critical research frontier. In view of this, several approaches have been introduced to modify biochar, thereby producing biochar with engineered structures, which improve the adsorption ability of biochar towards CO<sub>2</sub> sequestration. To enhance biochar adsorption capacity towards CO<sub>2</sub>, several

research groups have modified the synthetic procedure for the production of biochar with improved pore volume, specific surface area (SSA), surface functionality, and surface hydrophilicity, which improve the application scenarios of biochar.<sup>9,13</sup> In general, chemical and physical activation approaches were employed for the modification of biochar.<sup>9,14</sup> For instance, surface functionalization of biochar can be performed by oxidation of the biochar employing alkali reagents (*e.g.*, KOH, NaOH, *etc.*), introduction of an NH<sub>2</sub> group *via* amination of biochar and impregnation of biochar with a metal oxide solution such as Mg, Ca, K, Na, and others for doping of metals into the biochar structure.<sup>14,15</sup> Biochar can also be modified using organic compounds such as chitosan and carbonaceous materials such as GO and others. The physical modification typically involves heating of biochar with an oxidizing agent or under an activation atmosphere, with steam and CO<sub>2</sub> being the most common oxidizing agents. Therefore, engineered biochar can be used as a powerful CO<sub>2</sub> adsorbent due to its large microporous structure and surface area.

While several reviews exist on biochar's general applications in carbon capture,<sup>16–18</sup> a focused and systematic analysis of modification strategies specifically aimed at boosting CO<sub>2</sub> adsorption performance, particularly one that links synthesis protocols to tailored properties and mechanistic outcomes, remains less explored. This work aims to present a comprehensive and critical review of recent advancements in the development and production of biochar-based engineered materials to capture CO<sub>2</sub> from the atmosphere. The primary emphasis is on the synthesis and modification strategies for fabricating biochar and its composites, as well as their resulting adsorption properties, including selectivity, maximum capacity, reusability, and desorption efficiency. Additionally, the study provides a dedicated and in-depth exploration of the separation mechanisms utilized in various biochar-based techniques. Furthermore, the effectiveness of these materials is assessed based on their adsorption performance and selectivity. By establishing clear structure–property relationships, this review serves as a targeted guide for researchers and manufacturers designing next-generation, high-performance biochar-based adsorbents for potential industrial CO<sub>2</sub> capture applications.

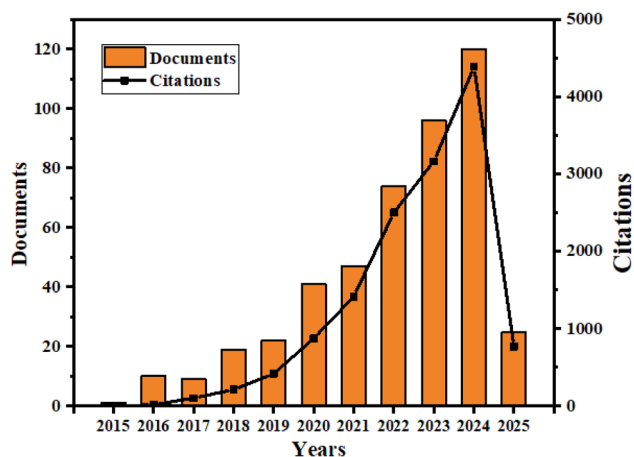


Fig. 1 Number of recent research literature reports on biochar adsorption of CO<sub>2</sub> (data from Scopus, 2015 to 2025).

## 2 CO<sub>2</sub> emissions and their effect on human health

Numerous studies have explored the impact of natural resource depletion on environmental and economic challenges associated with energy consumption.<sup>19</sup> Economic growth and the excessive use of natural resources play a major role in increasing CO<sub>2</sub> emissions.<sup>20</sup> The combustion of fossil fuels like oil, natural gas, and coal, along with biomass and solid waste, results in CO<sub>2</sub> emissions.<sup>21</sup> Human activities can also disrupt the carbon cycle, increasing CO<sub>2</sub> emission into the environment and affecting the capacity of natural carbon stores. The main source of man-made CO<sub>2</sub> emission is the burning of fossil fuels for power generation and transport, while certain changes in land use, such as deforestation, can contribute to CO<sub>2</sub>



emission.<sup>22</sup> Severe exposure to high concentrations of CO<sub>2</sub> in the atmosphere can have adverse effects on human health, including inducing inflammatory responses and affecting cognition.<sup>23</sup> Exposure to 3000 ppm of CO<sub>2</sub> can cause mild nasal inflammation in human, while levels of 5000 ppm have been linked to heightened bronchial epithelial inflammation in rats.<sup>24</sup> Furthermore, in mice, exposure to 5000 ppm CO<sub>2</sub> combined with organic swine dust in a dose-dependent manner may result in lung inflammation.<sup>14</sup> Thus, even at common environmental levels, CO<sub>2</sub> exposure can intensify inflammatory responses by altering the innate immunity.<sup>25</sup> On the International Space Station, high CO<sub>2</sub> levels have been linked to headaches, symptoms of sick building syndrome, decreased cognitive function, and increased student absenteeism.<sup>26</sup> According to two recent assessments, ecologically related CO<sub>2</sub> increase may have a direct effect on higher order cognitive functions like problem solving and decision making.<sup>27</sup>

### 3 Preparation and properties of biochar-based engineered materials

Biochar is typically produced from organic raw materials such as industrial, agricultural, and municipal waste, as well as algae biomass.<sup>28</sup> It is well known for its exceptional adsorption capacity, making it a highly effective adsorbent.<sup>29</sup> Moreover, using environmental waste streams as raw materials for biochar production supports the principles of sustainable development and circular bioeconomy, delivering significant positive impacts on environmental preservation.<sup>10</sup> In general, biochar is prepared using technologies including liquefaction, torrefaction, pyrolysis, gasification, and microwave synthesis. A comprehensive overview of these synthesis methods, their subsequent modifications, and related applications is presented in Fig. 2. The following section below will discuss biochar preparation methods and its properties.

#### 3.1 Pyrolysis

Biomass pyrolysis is a thermochemical process that breaks down biomass at temperatures between 300 and 900 °C under

limited or oxygen-free conditions.<sup>30</sup> Achieving a carbon content above 95% may necessitate treatment at higher temperatures >700 °C. This is achievable with woody feedstock, but it becomes more difficult with agricultural waste and other materials that generate ash at lower temperature. Consequently, these materials are usually not processed at temperatures exceeding 700 °C.<sup>31</sup> The pyrolysis process effectively transforms waste biomass into valuable products, including biochar, bio-oil, and syngas.<sup>32</sup> It is generally categorized into three types fast-, intermediate- and slow-pyrolysis based on factors such as reaction temperature, residence time and heating rate. Fast pyrolysis is mainly employed to produce bio-oil, thanks to its short residence time of under 2 seconds and high bio-oil yield, which can reach up to 75%.<sup>33</sup> Intermediate and slow pyrolysis processes, which involve longer residence times, are designed to maximize the production of solid biochar from various feedstocks. Biomass pyrolysis encompasses a range of thermal decomposition processes, making it challenging to define precisely. For example, in slow pyrolysis, biomass is heated gradually to approximately 500 °C in the absence of air, with vapor residence times ranging from 5 to 30 min. Slow pyrolysis generates low vapor as compared to rapid pyrolysis and typically results in a biochar yield of 25–35%.<sup>34</sup> Interestingly, it was noticed that higher solid yields were observed at slow heating rates and low operating temperatures in the process of slow pyrolysis.<sup>35</sup> For instance, Sawargaonkar *et al.* illustrated that higher yields of biochar were produced from peanut shell *via* slow pyrolysis, regardless of the reaction temperature, thus confirming the effectiveness of slow pyrolysis for biochar production.<sup>36</sup> Babu *et al.* used mixed wood waste to prepare biochar *via* slow pyrolysis at different temperatures (400, 600, and 800 °C) and holding times (30, 45, and 60 min).<sup>37</sup> Fig. 3 presents a schematic graphical layout of the experimental pyrolysis setup. Their results showed that the biochar yield decreased with increasing temperature from 400 to 800 °C but the carbon content increased. Higher pyrolysis temperatures (400–800 °C) led to higher bulk density and heating value. Additionally, both the Brunauer–Emmett–Teller (BET) surface area and zeta potential demonstrated notable enhancement within this temperature range. Field emission scanning

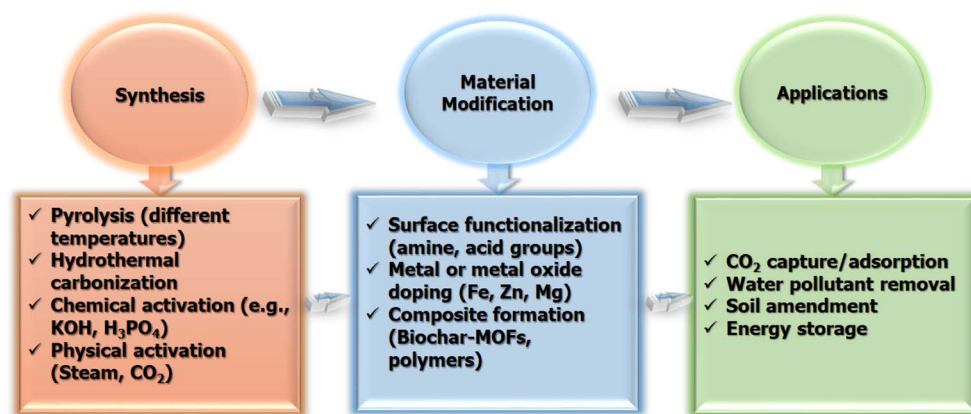


Fig. 2 Overview of biochar synthesis, modifications, and their application pathways.



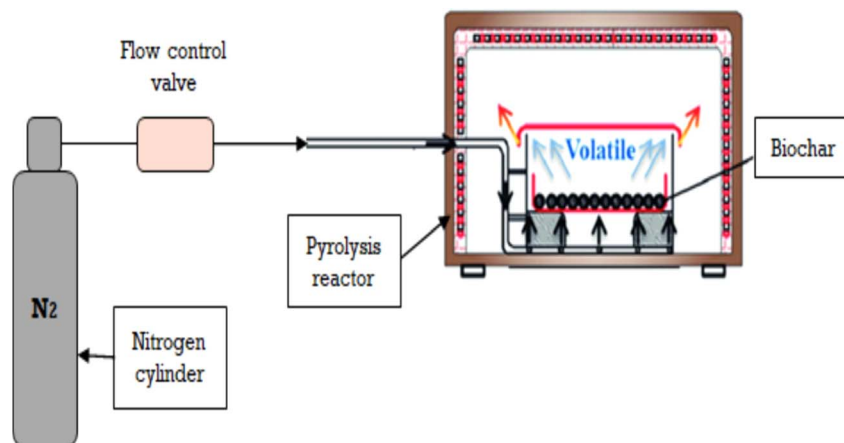


Fig. 3 The schematic representation of the experimental pyrolysis setup. Reproduced with permission from ref. 37. Copyright 2024 Elsevier, B. V.

electron microscopic (FE-SEM) data revealed that higher temperatures enhanced volatilization, leading to significant changes in the surface structure. Moreover, several studies have indicated that slow pyrolysis increases the concentration of oxygenated functional groups, especially carboxylic groups, in the biochar structure.<sup>38</sup> These increased carboxylic groups can enhance the capture of CO<sub>2</sub> from the atmosphere.<sup>9</sup>

### 3.2 Torrefaction

Torrefaction is considered the first stage in the pyrolysis process, taking place between 250 and 280 °C at relatively low heating rates. This process produces brown or black biochar with low mechanical strength. Nevertheless, torrefaction can generate wood yields of up to 84%, with maximum energy efficiency reaching 90%.<sup>39</sup> Torrefaction as a mode of valorisation improves the energy density of biomass, reduces its weight, increases its hydrophobicity and thus facilitates its commercial use by reducing transport, storage, and disposal problems.<sup>40</sup> This process has attracted considerable interest in various fields, particularly in bioenergy, where it is used as a pre-

treatment step to enhance the physicochemical properties of biomass.<sup>41</sup> Fig. 4 shows a schematic depiction of the different steps of the torrefaction process.

For example, Lampropoulos *et al.* prepared biochar from olive kernel biomass using a combination of torrefaction and pyrolysis.<sup>42</sup> The resulting biochar exhibited a more disordered structure, increased carbon and ash content, and enhanced porosity.<sup>42</sup> In another study, torrefaction was performed by using both water-washed rice straw and raw rice straw followed by pyrolysis.<sup>43</sup> The torrefaction temperatures were set at 200, 250, and 300 °C, while the pyrolysis temperatures were 800, 1000, and 1200 °C. The biochar produced from torrefied biomass exhibited improved adsorption efficiency compared to biochar obtained from untreated biomass, despite the observed decrease in SSA.<sup>43</sup> Mukherjee *et al.* carried out torrefaction on two types of biomass, namely coffee husks and spent coffee grounds, to produce biochar for CO<sub>2</sub> capture from the atmosphere.<sup>44</sup> The experiment was conducted at 200 °C, 250 °C, and 300 °C, with torrefaction times of 0.5 and 1 hour. The findings of this study showed that the carbon content was increased to 69.5 and 61.2% using spent coffee grounds and coffee husks as the carbon source by performing torrefaction at 300 °C for 60 min, while their oxygen content decreased significantly. Higher heating values also improved, reaching 25 MJ kg<sup>-1</sup> for coffee husks and 30.3 MJ kg<sup>-1</sup> for spent coffee grounds. In CO<sub>2</sub> capture tests, biochar from spent coffee grounds exhibited a higher CO<sub>2</sub> sorption capacity (0.38 mmol g<sup>-1</sup>) than coffee husks (0.23 mmol g<sup>-1</sup>). This was attributed to its more porous structure (10.4 × 10<sup>-3</sup> cm<sup>3</sup> g<sup>-1</sup>), larger surface area (100 m<sup>2</sup> g<sup>-1</sup>), and greater abundance of oxygenated functional groups.<sup>44</sup> Traditional torrefaction is typically performed under atmospheric conditions. However, recent studies have shown that conducting torrefaction in a pressurized gas environment can further enhance the properties and combustion performance of biomass.<sup>45</sup> For instance, Gao *et al.* investigated the effects of torrefaction pressure on the pyrolysis behavior of torrefied rice straw.<sup>46</sup> The pyrolysis of rice straw torrefied in a gas-pressurized autoclave was safer and the rice straw was more stable than that torrefied in a rotary tube reactor.<sup>46</sup>

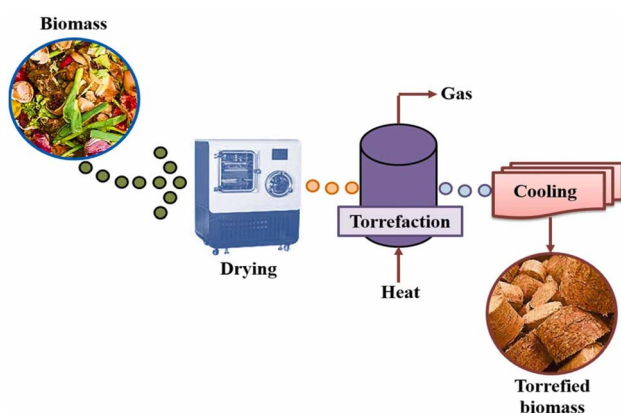


Fig. 4 Schematic representation of various stages of the torrefaction process. Reproduced with permission from ref. 39. Copyright 2024 Elsevier, B. V.



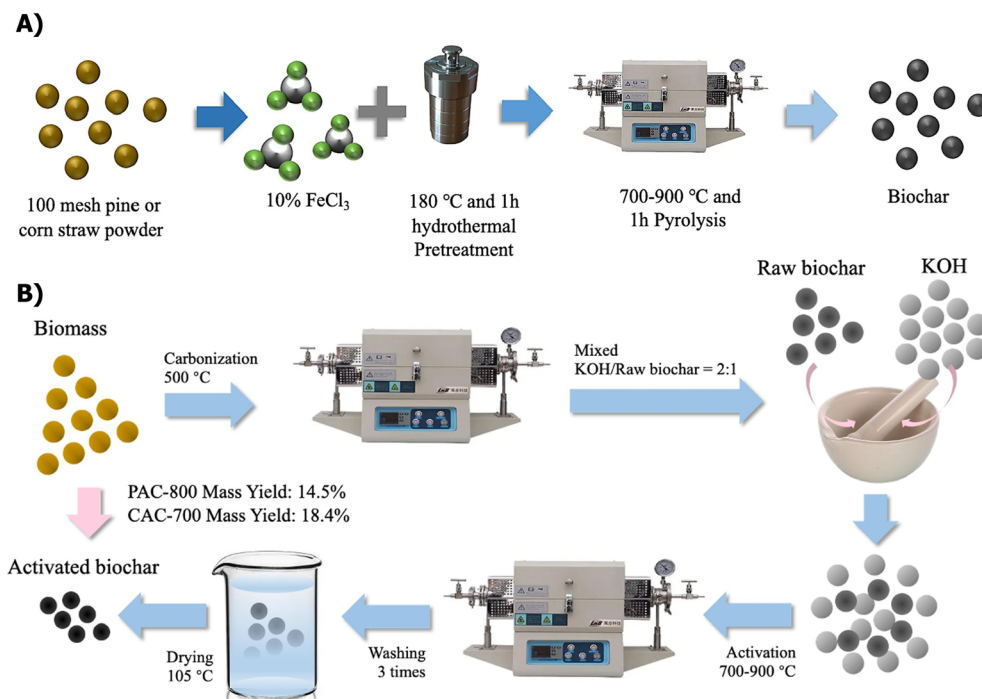


Fig. 5 (A) The flow chart of the biochar preparation from corn straw and pine branches. Reproduced with permission from ref. 54. Copyright 2024 Elsevier, B. V. and (B) flowchart of KOH-activated biochar preparation from pine and corn straw using the HTC process. Reproduced with permission from ref. 55. Copyright 2024 Elsevier, B. V.

### 3.3 Hydrothermal carbonization

Hydrothermal carbonization (HTC) is a wet thermochemical process where biomass is immersed in water inside a sealed Teflon-lined vessel and subjected to temperatures between 120 °C and 220 °C for several hours.<sup>47</sup> This process takes place under self-generated pressure, ensuring the reaction occurs in a water-saturated environment.<sup>48</sup> HTC is both spontaneous and exothermic, which helps maintain uniform carbon distribution in the final product.<sup>48</sup> Biochar obtained through this method tends to contain abundant oxygen-containing functional groups, enhancing its ability to adsorb various contaminants.<sup>49</sup> Moreover, HTC does not typically require extensive pre-treatment of raw materials, thereby reducing initial energy demands. However, longer processing times can lead to increased energy consumption, though the product yield is generally higher compared to some other conversion methods.<sup>50</sup> HTC also offers advantages such as low-temperature operation in aqueous media and the production of biochar with consistent chemical composition and structural features.<sup>51</sup> However, one notable drawback is the low porosity of the resulting biochar, which usually necessitates additional thermal activation at elevated temperatures.<sup>52</sup> The porosity enhancement process is often conducted under an inert atmosphere with chemical activators like KOH, NaOH, or H<sub>3</sub>PO<sub>4</sub>.<sup>53</sup> Both the activating agent used and the pyrolysis temperature influence the final pore structure and surface chemistry.<sup>50</sup> Overall, HTC presents itself as an efficient, cost-effective, and energy-conscious method for converting diverse biomass sources into functional biochar materials.<sup>53</sup>

For example, Zhang *et al.* described a hydrothermal treatment approach for biochar from corn straw and pine through hydrothermal pretreatment.<sup>54</sup> The biochar production process is illustrated in Fig. 5A. Their findings indicated that the SSA of pine and corn straw biochar reached 397.86 m<sup>2</sup> g<sup>-1</sup> and 448.24 m<sup>2</sup> g<sup>-1</sup>, respectively. Among the tested samples, pine biochar fabricated at 700 °C showed superior CO<sub>2</sub> adsorption capacity (5.35 wt%) and high removal efficiency at room temperature. The captured CO<sub>2</sub> interacted with the biochar composites, forming active functional groups, which facilitated the release of free radical oxygen, enhancing CO<sub>2</sub> removal efficiency.<sup>54</sup> The same research group utilized HTC to prepare KOH-activated biochar from pine and corn straw for capturing CO<sub>2</sub>.<sup>55</sup> The activation procedure is illustrated in Fig. 5B. Their findings revealed that elevating the activation temperature notably improved the SSA of the biochar. Among the samples, pine-derived biochar treated at 800 °C demonstrated the highest CO<sub>2</sub> adsorption capacity, achieving 3.79 mmol g<sup>-1</sup> at 25 °C.<sup>55</sup> Recently, Liu *et al.* synthesized nitrogen-doped biochar (CNPBs) with porous structures from discarded cigarette butts, employing mixed salts as doping agents and ammonium sulfate as the nitrogen source.<sup>56</sup> The synthesis involved HTC followed by mild pyrolytic activation. Among the prepared materials, CNPB-2-600 (biochar produced at 600 °C with a KOH ratio of 2) exhibited remarkable CO<sub>2</sub> adsorption properties, achieving 4.93 mmol g<sup>-1</sup> at 1 bar and 25 °C and 6.83 mmol g<sup>-1</sup> at 0 °C. Additionally, it demonstrated high selectivity (CO<sub>2</sub>/N<sub>2</sub> = 23.4 at 1 bar and 25 °C), excellent recyclability (95.33% retention over five cycles), and outstanding dynamic CO<sub>2</sub> uptake (1.67 mmol g<sup>-1</sup> at 1 bar and 25 °C).<sup>56</sup>



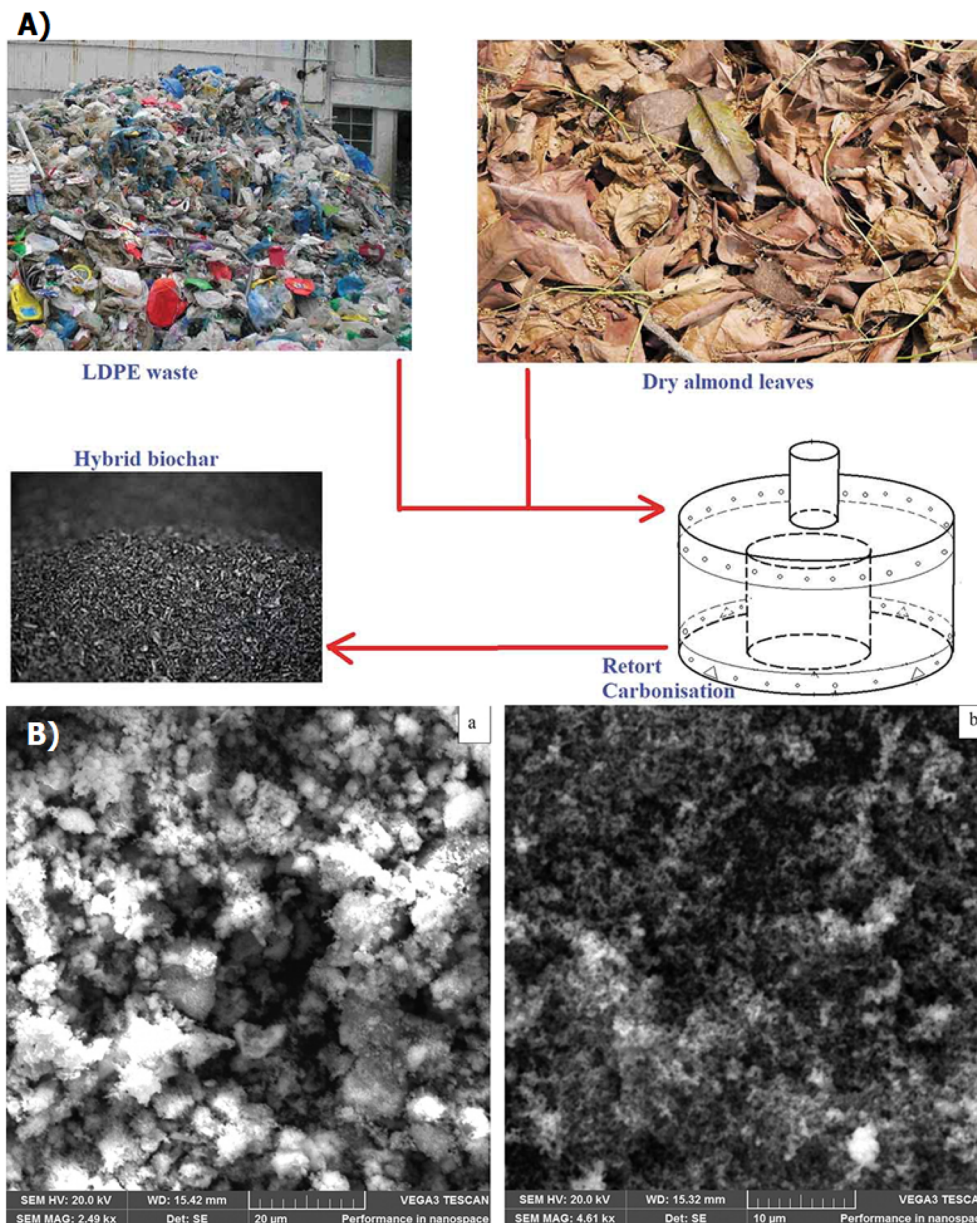


Fig. 6 Biochar production and structural analysis: (A) conversion of dry almond (*Terminalia catappa*) leaves and LDPE waste into biochar using a low-temperature, char-optimized process and (B) SEM micrographs of (a) biomass biochar and (b) hybrid biochar derived from almond (*Terminalia catappa*) leaves and LDPE waste.<sup>61</sup>

### 3.4 Gasification

Gasification differs significantly from pyrolysis due to its much higher temperature.<sup>57</sup> It refers to the partial breakdown of biomass at elevated temperatures (600–1200 °C) with a brief residence time of 10 to 20 seconds.<sup>58</sup> Gasification is mainly used to produce a gas-fuel which can be used to produce heat or electricity and biochar. Several influencing parameters such as gas composition, particle size, residence time and reaction temperature were optimized to control the reaction for the formation of engineered biochar. This technique produces a minimal amount of biochar, as the majority of the material is transformed into gas and ash. Depending on the process

conditions, the final biochar yield could be less than 10%.<sup>59</sup> Toxic compounds, including alkali and alkaline earth metals as well as polyaromatic hydrocarbons, are commonly found due to the elevated reaction temperature.<sup>60</sup> For instance, Ighalo *et al.* investigated the retort-heating carbonization of *Terminalia catappa* (almond) leaves and low-density polyethylene (LDPE) waste for engineered biochar formation, evaluating the quality of the resulting material.<sup>61</sup> Fig. 6A illustrates the preparation of biochar from leaves of dry almond and LDPE waste using a low-temperature, char-optimized gasification process. The results showed that biomass biochar achieved a yield of 28.57 wt%, while hybrid biochar (from almond leaves and LDPE) reached 71.43 wt%, outperforming similar biomass feedstocks. The



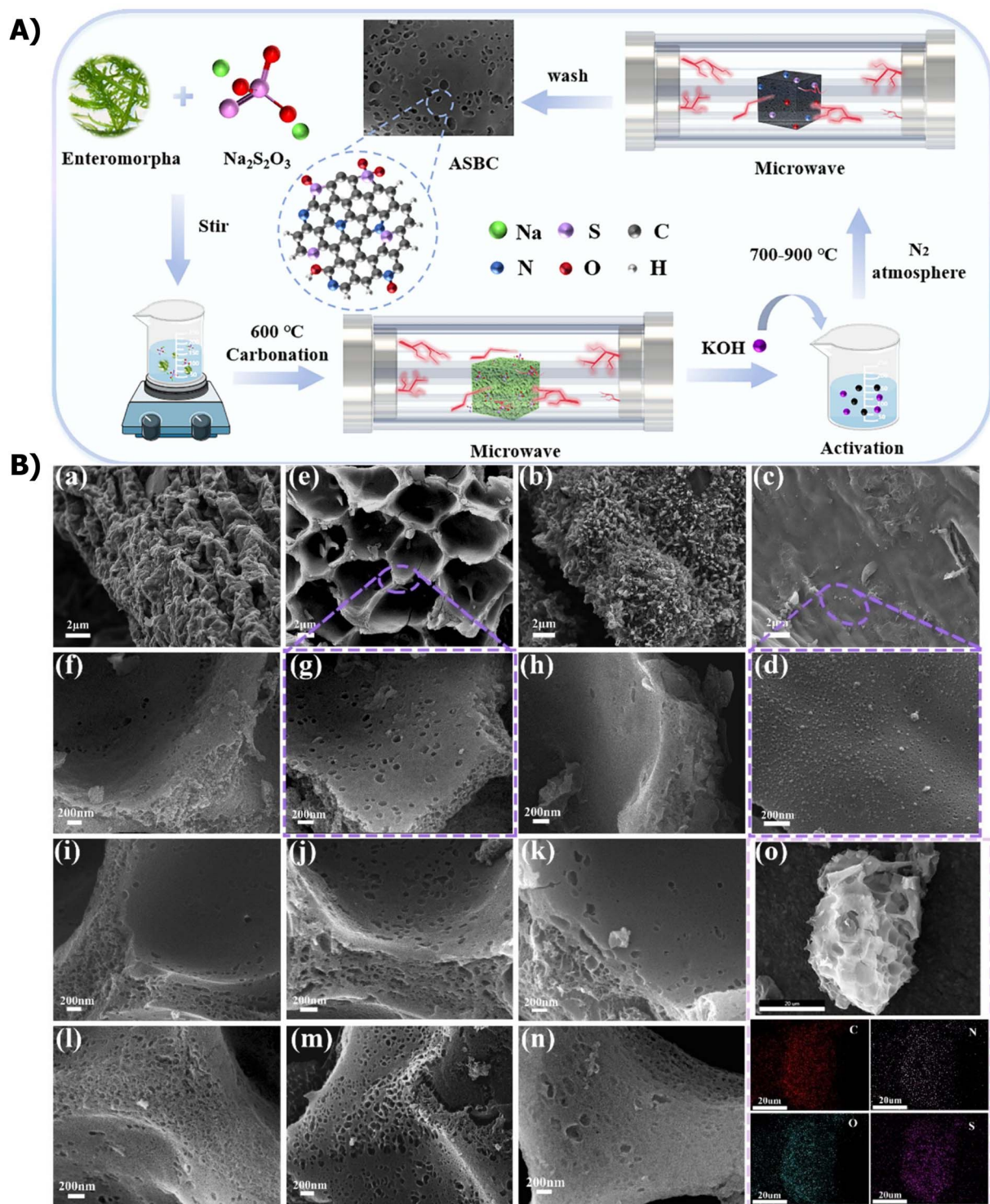


Fig. 7 (A) Schematic of N, S co-doped porous biochar preparation via microwave-assisted carbonization for CO<sub>2</sub> removal and (B) SEM images of EBC (a), ESBC (b), ABC-700-0 (c and d), ASBC-700-0.5 (e and g), ASBC-700-0.25 (f), ASBC-700-1 (h), ASBC-800-0.25 (i), ASBC-800-0.5 (j), ASBC-800-1 (k), ASBC-900-0.25 (l), ASBC-900-0.5 (m), ASBC-900-1 (n) and EDS images of ASBC-800-0.5 (o). Reproduced with permission from ref. 70. Copyright 2024 Elsevier, B. V.

peak temperatures were 494 °C for biomass biochar and 362 °C for hybrid biochar, with a total processing time of 90 min. SEM images demonstrated that the as-prepared biochar had smaller voids, whereas hybrid biochar exhibited a heterogeneous

morphology with minimal voids (Fig. 6B). BET analysis indicated mesoporous structures with surface areas of 450.2 m<sup>2</sup> g<sup>-1</sup> for biomass biochar and 296.8 m<sup>2</sup> g<sup>-1</sup> for hybrid biochar.<sup>61</sup> In recent years, limited research has explored the use of gasified



biochar for CO<sub>2</sub> capture.<sup>62</sup> For example, Dissanayake *et al.* synthesized biochar through the gasification of wood chips and chicken manure, achieving measurable adsorption capacity (2.92 mmol g<sup>-1</sup>).<sup>63</sup> In another study, Nguyen *et al.* utilized various biomass sources, including bagasse, bamboo, and rice husk, to produce biochar *via* gasification for CO<sub>2</sub> removal.<sup>62</sup> The biochar exhibited significant CO<sub>2</sub> adsorption, with uptake reaching up to 9.5 wt% at 25 °C and 1 atm. Additionally, it demonstrated remarkable recyclability, maintaining performance after 30 cycles and exposure to moisture.<sup>62</sup> The presence of oxygen-rich functional groups and aromatic structures in gasified biochar enhances its adsorption potential.<sup>16</sup>

### 3.5 Microwave-assisted carbonization

The increasing environmental awareness has driven research toward the development of efficient recycling and waste recovery methods.<sup>64</sup> Microwave-assisted biochar preparation is considered one of the most effective and cost-efficient methods for synthesizing biochar adsorbents. This approach serves as an alternative heating source for converting organic waste biomass into valuable solid products such as activated carbon, hydrochar, and biochar. Compared to conventional heating, microwave-assisted carbonization offers a more rapid and efficient process, providing uniform, selective, and non-contact heating.<sup>65</sup> This advantage arises from its heating mechanism, which is based on energy transfer rather than heat transfer. As a result, microwave-assisted carbonization overcomes the drawbacks of conventional heating methods, including prolonged processing time, radiative heat loss and uneven heat distribution.<sup>66</sup> Due to these unique characteristics, microwave-assisted carbonization can enhance reaction selectivity, improve process efficiency, and enable chemical reactions that may not occur under conventional heating conditions.<sup>67</sup> For instance, studies have reported that the biochar produced from rice straw *via* microwave pyrolysis exhibited higher CO<sub>2</sub> adsorption capacity, which is comparable to that of activated carbon.<sup>68</sup> Therefore, microwave-assisted carbonization of biomass waste presents a viable and energy-efficient approach for producing high-performance biochar with significant CO<sub>2</sub> adsorption capacity while minimizing energy consumption, cost, and processing time. For example, Huang *et al.* investigated the production of biochar through microwave-assisted copyrolysis of sewage sludge and leucaena wood for CO<sub>2</sub> capture.<sup>69</sup> The biochar produced under optimal conditions, specifically at a microwave power level of 150 W with 25% sewage sludge content, achieved the highest CO<sub>2</sub> adsorption capacity of 0.95 mmol g<sup>-1</sup>.<sup>69</sup> Similarly, Chen and co-workers used microwave pyrolysis to prepare a series of N, S co-doped biochars by adding an external sulfur source, with Enteromorpha serving as both the nitrogen source and carbon precursor.<sup>70</sup> It was confirmed that N, S co-doped biochar involves two key processes (carbonization and activation) (Fig. 7A). The results showed that the CO<sub>2</sub> adsorption capacity was increased from 2.84 to 2.95 mmol g<sup>-1</sup> with the use of dual-doped biochar. This enhancement in CO<sub>2</sub> adsorption was attributed to the improved balance between the active functional groups of engineered

biochar and pore structure, which could be adjusted by varying the amount of sulfur doping (Fig. 7B). In another study, bamboo biochar was modified through lignin impregnation followed by microwave irradiation to enhance CO<sub>2</sub> removal.<sup>71</sup> The authors found that the impregnation ratio significantly influenced the biochar's pore structure. The biochar with a lignin-to-biochar mass ratio of 1 : 20 exhibited the highest SSA of 377.32 m<sup>2</sup> g<sup>-1</sup> and a micropore volume of 0.163 cm<sup>3</sup> g<sup>-1</sup>. Lignin impregnation improved the CO<sub>2</sub> adsorption capacity of the biochar, reaching 3.05 mmol g<sup>-1</sup>.<sup>71</sup>

## 4 Analytical techniques for characterization of biochar

The effective design of biochar for CO<sub>2</sub> adsorption requires a systematic characterization strategy to link its physicochemical properties to its adsorption performance. For researchers targeting CO<sub>2</sub> capture, a logical characterization sequence begins with fundamental composition analysis, proceeds to the critical textural properties governing physisorption, and culminates in surface chemistry analysis.

The initial and essential step involves proximate and ultimate analysis. Proximate analysis determines the biochar's moisture, ash, volatile matter, and fixed carbon content. The ash content, determined by combustion at approximately 730 °C, is particularly significant. Premchand *et al.* (2023) reported that biochar ash produced in a nitrogen atmosphere is always lower than that produced in a CO<sub>2</sub> atmosphere.<sup>72</sup> For CO<sub>2</sub> adsorption, a higher ash content can be favorable if the ash is alkaline (rich in K<sub>2</sub>O and CaO), as the basic sites attract acidic CO<sub>2</sub> molecules.<sup>72</sup> However, inert ash can block pore access. Ultimate (elemental) analysis defines the content of carbon (C), hydrogen (H), nitrogen (N), oxygen (O), and sulfur (S). Atomic ratios (O/C, H/C, (O + N)/C) provide insight into the degree of carbonization, aromaticity, polarity, and hydrophobicity.

The most critical properties for CO<sub>2</sub> physisorption are textural, specifically the ultramicroporous structure. N<sub>2</sub> physisorption at 77 K is the standard method to determine the SSA and pore volume.<sup>73</sup> However, for CO<sub>2</sub> capture, CO<sub>2</sub> physisorption at 0 °C or 25 °C is indispensable, as it accurately probes the narrow ultramicropores (<0.8 nm) that are optimal for capturing CO<sub>2</sub> molecules under ambient conditions but are often inaccessible to N<sub>2</sub> at 77 K due to diffusion limitations. The direct measurement of CO<sub>2</sub> uptake under relevant conditions (*e.g.*, 1 bar, 25 °C) is the key performance metric.

Surface chemistry characterization elucidates the mechanisms of enhanced adsorption. X-ray photoelectron spectroscopy (XPS) is highly recommended, as it provides quantitative information about the elements and functional groups (*e.g.*, pyrrolic/pyridinic N, C=O, C-O, Ca<sup>2+</sup>) present on the biochar surface before and after adsorption.<sup>74</sup> Fourier transform infrared spectroscopy (FTIR) complements this by identifying bulk functional groups related to surface polarity and basicity. SEM visualizes changes in surface morphology and pore structure resulting from synthesis or activation treatments.<sup>9</sup>



Additional techniques provide valuable supporting information. Thermogravimetric analysis (TGA) confirms thermal stability, while Boehm titration quantifies acidic and basic surface functional groups. Zeta potential measurements determine the surface charge, influencing the interactions with CO<sub>2</sub>.<sup>75</sup> Raman spectroscopy, through its D and G bands, analyzes the graphitic disorder and carbon structure in the biochar.<sup>76</sup> Energy dispersive X-ray spectroscopy (EDX), X-ray fluorescence (XRF), and nuclear magnetic resonance (NMR) can also be used for elemental and structural analysis. In summary, the adsorption of CO<sub>2</sub> by biochar is governed by a synergistic interplay of narrow micropore volume (texture) and basic surface functional groups or inorganic species. A characterization protocol integrating both aspects is essential for rational adsorbent design.

## 5 Application of unmodified biochar and biochar-based engineered materials in CO<sub>2</sub> elimination

Over the past decade, significant efforts have been made to modernize CO<sub>2</sub>-emitting industrial processes, particularly in East Asia and North American countries, which are among the largest contributors to greenhouse gas emissions. Many countries have strengthened environmental regulations on atmospheric emissions and adopted more efficient energy policies, driving an energy transition towards renewable and green energies, in line with Sustainable Development Goals (SDGs).<sup>77</sup> However, due to various challenges, achieving this transition in the short term remain difficult, highlighting the need for direct CO<sub>2</sub> capture from major emission sources.

A wide range of techniques are available for this purpose, including: (i) pre-combustion capture techniques, using fuel gasification for subsequent production of syngas (CO and H<sub>2</sub>), which is then treated for CO<sub>2</sub> separation.<sup>78</sup> Although this technique leads to high-purity CO<sub>2</sub>, it demands a substantial initial investment due to the complexity of the equipment required for gasification and associated conversion reactions;<sup>79</sup> (ii) oxy combustion-based process in a high-oxygen-content atmosphere, leading to a combustion gas composed mainly of CO<sub>2</sub> and water steam, enabling a subsequent separation. However, this process requires a high energy input; (iii) chemical loop combustion techniques, generally using a metal oxide as an oxygen carrier to oxidize the fuel and generate energy, following repetitive redox cycles, producing thus pure CO<sub>2</sub>.<sup>80</sup> This process is still being studied under pilot scale demonstration and requires further testing for operationalization toward an efficient industrial application; and (iv) post-combustion capture techniques,<sup>81</sup> frequently by absorption on amine solvents, which consequently leads to recovery and purification challenges<sup>82</sup> as well as corrosion issues of the associated installations,<sup>83</sup> by cryogenic distillation which, besides the corresponding energy input, is still limited owing to selectivity restrictions as a function of operating temperature and pressure when using mixtures (*e.g.*, CO<sub>2</sub>/CH<sub>4</sub> mixtures),<sup>84</sup> by membrane separation, still under intensive research in order to overcome

limitations in terms of selectivity, permeability and membrane durability, as well as the technology cost (from manufacturing to dumping and/or recycling), or by physical adsorption on porous materials (activated carbon, zeolites, MOFs, *etc.*)<sup>85</sup> and chemical adsorption by means of tailored surface chemistry.<sup>86</sup> In short, adsorption on solid materials is among the most promising CO<sub>2</sub> capture technologies, mainly due to low energy consumption.<sup>87</sup> The process becomes even more cost-effective when low-cost materials are utilized. In this context, biochar represents a promising alternative to conventional adsorbents, offering a viable and versatile solution for CO<sub>2</sub> capture while contributing to climate change mitigation through the sustainable management of municipal solid waste. To minimize energy penalties, biochar can be synthesized from inexpensive precursors such as biomass and easily scaled up,<sup>88</sup> enabling its integration into environmentally friendly concepts, particularly those aimed at reducing harmful emissions.<sup>89</sup> Biochar production typically involves carbonization processes,<sup>90</sup> which can be tailored to achieve the desired porous texture through physical or chemical activation, or surface modification (*e.g.*, introducing surface N-groups (pyridine, pyrrolic, graphitic, and oxidized pyridine)).<sup>88</sup> The effectiveness of biochar-based materials for CO<sub>2</sub> capture and storage depends on factors such as adsorption capacity, CO<sub>2</sub>/N<sub>2</sub> selectivity, adsorption-desorption kinetics, regenerability, and cost. In the last decade, extensive research has focused on synthesizing biochar with an optimized porous structure specifically for CO<sub>2</sub> capture. These studies explore both the direct synthesis of tailored biochar (pristine biochar) and additional modifications to enhance adsorption performance under diverse operating conditions, including variation in temperatures, pressures, gas compositions, and humidity levels. In the following subsection, we will discuss recent applications of biochar and biochar-based materials for CO<sub>2</sub> capture from the atmosphere.

### 5.1 Unmodified biochar

Recently, biochar has attracted considerable interest as a sustainable carbon-based material for CO<sub>2</sub> capture, owing to its eco-friendly characteristics, cost-effective synthesis, and efficient adsorption capabilities.<sup>91</sup> Furthermore, the well-developed pore structure of biochar is essential for effective CO<sub>2</sub> adsorption through physical mechanisms.<sup>91</sup> The micropores of biochar, particularly those with diameters smaller than 1 nm, closely match the dynamic diameter of CO<sub>2</sub> molecules.<sup>92</sup> Additionally, the interaction between adjacent pore walls strengthens the adsorption forces, improving CO<sub>2</sub> capture efficiency.<sup>93</sup> As a result, optimizing the pore distribution of biochar can enhance its physical adsorption capacity. Table 1 provides detailed information on synthesis methodologies, surface area analysis, pore volume, and adsorption properties.

For instance, a porous biochar was prepared from softwood biomass *via* the pyrolysis method under an inert atmosphere at 500 °C for CO<sub>2</sub> removal.<sup>94</sup> The biochar's CO<sub>2</sub> adsorption capacity was assessed under the identical pressure conditions but at slightly lower temperatures, around 20 °C. The maximum adsorption capacity of sawmill residue-based biochar reached



Table 1 A summary of previous studies on unmodified biochar for CO<sub>2</sub> capture

Feedstock	Thermal process	Porosity/surface characteristic-enhancing process	SSA <sup>a</sup> (m <sup>2</sup> g <sup>-1</sup> )	V <sub>t</sub> <sup>b</sup> (cm <sup>3</sup> g <sup>-1</sup> )	V <sub>0</sub> <sup>c</sup> (cm <sup>3</sup> g <sup>-1</sup> )	APS <sup>d</sup> (nm)	MF <sup>e</sup> (%)	T (°C)	P (bar)	CO <sub>2</sub> uptake <sup>f</sup> (mmol g <sup>-1</sup> )	(CO <sub>2</sub> /N <sub>2</sub> ) uptake ratio	Reference
Sawmill residues	Fast pyrolysis	—	95.58	—	0.03	4.36	—	20	1	2.4	—	94
Sewage sludge & <i>Leucaena</i> wood	Microwave co-torrefaction	—	—	—	—	—	—	—	—	1.2	—	102
Pecan nut shell	Microwave pyrolysis	—	187	0.08	0.07	—	—	25	1-1.2	2	∞	97
Spent coffee grounds	Slow pyrolysis	—	539	0.32	—	3.2	—	30	1	2.8	—	98
MgAl-layered double hydroxide & microcrystalline cellulose	Calcination	—	—	—	—	—	—	25	1	1.24	—	99
Chitosan	Two-stage slow pyrolysis of freeze-dried chitosan	—	<19	<0.05	—	—	—	25	~9	~2.4	~13	100
Softwood shavings	Fast pyrolysis	—	48.85	0.03	—	7.09	—	25	1	1.98	—	95
	Pyrolysis of sewage sludge pre-conditioned using CPAM <sup>g</sup>	—	40.1	0.02	0.02	3.06	—	30	—	1.1	—	101
	Steam assisted slow pyrolysis of cellulose fibers	—	593.0	0.25	0.25	—	—	25	1	2.33	21	111
	Acid-washing assisted by ultrasonic-treatment	—	1134	0.84	0.49	1.49	57	0	1	4.06	—	145
Date palm leaf waste	Fast pyrolysis	—	—	—	—	—	—	25	—	~5.68	—	96
Alkali lignin	Negative pressure pyrolysis	Acid-washing assisted by ultrasonic-treatment	1577	1.43	0.695	1.81	—	0	1	3.62	—	114
Softwood shavings	Fast pyrolysis	—	—	—	—	—	—	20	1	2325	—	154

<sup>a</sup> Specific surface area: calculated using the BET method. <sup>b</sup> Total pore volume obtained from the amount of N<sub>2</sub> adsorbed at  $p/p_0 \approx 0.95$ . <sup>c</sup> Micropore volume calculated by applying the DR equation to N<sub>2</sub> at -196 °C. <sup>d</sup> Average pore size. <sup>e</sup> Microporous fraction. <sup>f</sup> Deduced from CO<sub>2</sub> adsorption isotherms. <sup>g</sup> Cationic polyacrylamide.

2.4 mmol g<sup>-1</sup>, surpassing that of commercial zeolite-13<sup>X</sup> (1.7 mmol g<sup>-1</sup>). The Freundlich isotherm better predicted the experimental results than the Langmuir isotherm, suggesting that the sawmill residue-based biochar possessed a highly heterogeneous surface, enabling multilayer adsorption.<sup>94</sup> Likewise, Mamaghani *et al.* prepared biochar from softwood, which demonstrated a surface area of 48.85 m<sup>2</sup> g<sup>-1</sup>. The CO<sub>2</sub> adsorption was analyzed under different operating conditions (dry or wet), demonstrating consistent performance independent of humidity. The Avrami kinetic model effectively described the experimental adsorption data acquired under dry and wet conditions,<sup>95</sup> highlighting the potential of biochar for post-combustion CO<sub>2</sub> capture on an industrial scale.<sup>94</sup> In a separate study, Salem *et al.* produced date palm leaf biochar at temperatures of 300, 400, 500, and 600 °C, observing an increase in CO<sub>2</sub> adsorption from 0.09 to 0.25 kg CO<sub>2</sub> kg<sup>-1</sup> biochar as the temperature increased.<sup>96</sup> The findings also indicated that the CO<sub>2</sub> capturing ability of biochar was greatly improved by using biochar prepared at higher temperature because of the enhanced carbon content in the biochar.<sup>96</sup> Likewise, pecan shell-based biochar, produced *via* microwave pyrolysis, demonstrated an adsorption capacity of approximately 2 mmol g<sup>-1</sup> at 25 °C and 1–1.2 bar, with remarkably high CO<sub>2</sub>/N<sub>2</sub> selectivity.<sup>97</sup> This material (SSA = 187 m<sup>2</sup> g<sup>-1</sup>) displayed a highly microporous texture ( $V_0 = 0.066 \text{ cm}^3 \text{ g}^{-1}$  versus  $V_t = 0.075 \text{ cm}^3 \text{ g}^{-1}$ ) with a narrow ultra-micropore size distribution (~0.7 nm) and required no post-synthesis modification.<sup>97</sup> However, such a porous texture should be complemented by surface chemistry tailored to the intended application. This was confirmed by Alivia Mukherjee *et al.*,<sup>98</sup> who studied coffee-based biomass biochars produced through the slow pyrolysis process (SSA = 539 m<sup>2</sup> g;  $V_t = 0.32 \text{ cm}^3 \text{ g}^{-1}$ ). Their effective CO<sub>2</sub> adsorption capacity (approximately 3 mmol g<sup>-1</sup> at 30 °C and 1 bar) was attributed to a combination of microporous texture and the presence of (N-6) N-pyridinic and/or (N-5) N-pyridonic species.<sup>98</sup>

Tarmizi Taher *et al.* prepared layered double oxide (LDO)-cellulose-based biochar by simultaneously calcining layered double hydroxide (LDH) and microcrystalline cellulose, eliminating the need for post-synthesis modifications.<sup>99</sup> This biochar exhibited a CO<sub>2</sub> adsorption capacity of 1.24 mmol g<sup>-1</sup> at 25 °C and 1 bar. The incorporation of LDO into the biochar surface significantly improved its performance. Further characterization of the porous texture could establish correlations between the different structural properties and CO<sub>2</sub> capture optimization.<sup>99</sup> Additionally, Lourenço *et al.* developed a chitosan-based sponge-like biochar using chitosan freeze-drying followed by two-step pyrolysis.<sup>100</sup> This material achieved an adsorption capacity of approximately 2.4 mmol g<sup>-1</sup> at 25 °C and 9 bar, with a CO<sub>2</sub>/N<sub>2</sub> selectivity of about 13, confirming its high ultra-microporous texture.<sup>100</sup> Ghanbarpour Mamaghani *et al.* designed softwood-derived biochars using fast pyrolysis, achieving a CO<sub>2</sub> adsorption capacity of around 2 mmol g<sup>-1</sup> at 25 °C and 1 bar.<sup>95</sup> The non-activated softwood-derived biochars exhibited a surface area of 48.85 m<sup>2</sup> g<sup>-1</sup>. CO<sub>2</sub> adsorption analysis under different conditions (dry or wet) showed a stable performance, again validated by the Avrami kinetic model.<sup>95</sup>

With increasing global sewage sludge production, efficient treatment and disposal solutions are needed. Biochar production offers a viable alternative for managing sewage sludge. Its excellent chemical and physical features make sludge-derived biochar a promising CO<sub>2</sub> adsorbent.<sup>91</sup> For example, Liu *et al.* produced biochar from sewage sludge at 600 °C.<sup>101</sup> The raw sludge was treated by two common dehydration regulators (poly aluminum chloride and polyacrylamide), which notably enhanced the micropore volume and surface area to 0.022 cm<sup>3</sup> g<sup>-1</sup> and 40.1 m<sup>2</sup> g<sup>-1</sup>, and 0.025 cm<sup>3</sup> g<sup>-1</sup> and 41.2 m<sup>2</sup> g<sup>-1</sup>, respectively.<sup>101</sup> In another study, Huang *et al.* fabricated an effective biochar from leucaena wood and sewage sludge at different mixing ratios (75:25, 50:50, and 25:75) using microwave-assisted torrefaction at 250 W.<sup>102</sup> The findings indicated that pure leucaena wood biochar (1.2 mmol g<sup>-1</sup>) had nearly four times the adsorption capacity of pure sewage sludge biochar.<sup>102</sup>

Recently, researchers have explored replacing N<sub>2</sub> with CO<sub>2</sub> as a carrier gas during biomass pyrolysis. For instance, Godlewska *et al.* studied the pyrolysis characteristics of sewage sludge under CO<sub>2</sub> at 500, 600, and 700 °C, finding that CO<sub>2</sub> enhanced the aromatic properties of biochar.<sup>103</sup> Similarly Konczak *et al.* co-pyrolyzed sludge with CO<sub>2</sub>, effectively reducing biochar toxicity and mitigating the greenhouse effect.<sup>104</sup> Although modification strategies enhance the performance of biochar, they also increase production costs and resource consumption. Thus, developing cost-effective sludge biochar modification approaches remains a key research direction. In a related but distinct application, the CO<sub>2</sub> adsorption capacity of biochar has been well established in multiple studies. However, real-world CO<sub>2</sub> emissions are rarely pure. Understanding the effect of gas mixtures on CO<sub>2</sub> adsorption is crucial. One common associated gas is CO. Recently, Mamaghani *et al.* prepared biochar from softwood using fast pyrolysis at 500 °C for CO and CO<sub>2</sub> capture.<sup>105</sup> It was observed that pure CO<sub>2</sub> (2.325 mmol g<sup>-1</sup>) showed higher adsorption as compared to pure CO (0.700 mmol g<sup>-1</sup>). The Avrami kinetic model best described the adsorption process, indicating the involvement of both chemical and physical adsorption mechanisms.<sup>105</sup>

## 5.2 Biochar-based engineered materials

Biochars can be modified through pre- or post-synthesis treatments to optimize their surface properties, including physical characteristics like surface area, pore volume, and microporosity, as well as surface chemistry, which involves acidic, basic, and neutral functional groups essential for CO<sub>2</sub> adsorption.<sup>13</sup> The most commonly used biochar modification techniques include physical, chemical, and biological modifications. Table 2 provides detailed information on synthesis methodologies, pore volume data, sorption characteristics and surface area measurements, along with comprehensive examples of modified biochar.

**5.2.1 Physical modification.** Physical treatment generally includes thermally activating biochar with an oxidizing agent, commonly using steam or CO<sub>2</sub>.<sup>9</sup> Activation with CO<sub>2</sub> or steam introduces oxygen-containing functional groups onto the



Table 2 A summary of previous studies on physical modifications of biochar for CO<sub>2</sub> capture

Feed stock	Thermal process	Porosity/surface characteristic-enhancing process	SSA <sup>a</sup> (m <sup>2</sup> g <sup>-1</sup> )	V <sub>t</sub> <sup>b</sup> (cm <sup>3</sup> g <sup>-1</sup> )	V <sub>0</sub> <sup>c</sup> (cm <sup>3</sup> g <sup>-1</sup> )	APS <sup>d</sup> (nm)	T (°C)	P (bar)	CO <sub>2</sub> uptake <sup>e</sup> (mmol g <sup>-1</sup> )	(CO <sub>2</sub> /N <sub>2</sub> ) uptake ratio	Reference
Paper mill sludge and pine sawdust	Slow pyrolysis	Steam activation	581.7	0.25	—	2.24	25	1	2.49	26.7	110
Palm kernel shell	Carbonization	CO <sub>2</sub> activation	547.1	0.34	0.22	2474	25	1	2.5	—	109
<i>Populus nigra</i> wood & cellulose fibers	Slow pyrolysis	Steam assisted slow pyrolysis of cellulose fibers	593.0	0.25	0.25	—	25	1	2.33	21	111
Date seeds	Slow pyrolysis	CO <sub>2</sub> activation	798.4	—	0.28	—	25	1	2.94	—	112
Agricultural wastes	Slow pyrolysis	CO <sub>2</sub> activation of vine shoots	536	—	0.16	—	25	0.14	1.16	50	113
Rice husk	Fast pyrolysis	CO <sub>2</sub> activation	1097	~0.83	0.34	—	25	1	3.1	7.6	146

<sup>a</sup> Specific surface area: calculated using the BET method. <sup>b</sup> Total pore volume obtained from the amount of N<sub>2</sub> adsorbed at  $p/p_0 \approx 0.95$ . <sup>c</sup> Micropore volume calculated by applying the DR equation to N<sub>2</sub> at -196 °C. <sup>d</sup> Average pore size. <sup>e</sup> Deduced from CO<sub>2</sub> adsorption isotherms.

biochar surface, originating from the oxygen in CO<sub>2</sub> and water vapor (H<sub>2</sub>O).<sup>106</sup> Steam, having a smaller molecular size, can penetrate the biochar's porous structure more efficiently, resulting in a faster reaction rate and a higher concentration of predominantly acidic oxygen-containing functional groups.<sup>107</sup> The types of oxygen-containing functional groups introduced by CO<sub>2</sub> and steam activation differ. CO<sub>2</sub> activation tends to eliminate C=O and O-H groups, whereas steam activation promotes the formation of phenolic and COOH groups.<sup>108</sup> It is well known that the number of -COOH and phenolic groups were increased in biochar by the steam activation process, favoring the increase of the polarity and hydrophilicity of biochar. Biochar prepared from physical treatment with steam or CO<sub>2</sub> was found to be more efficient for industrial-scale applications as compared to the biochar prepared from chemical treatment. It avoids the use of chemicals, making it eco-friendly, and is cost-effective and free from secondary pollution. Additionally, it is time-efficient and produces biochar with fewer impurities.<sup>109</sup> Table 2 provides detailed information on synthesis methodologies, pore volume data, surface area measurements, and sorption characteristics, along with comprehensive examples of modified biochar. "Oxygen from H<sub>2</sub>O interacts with carbon surface sites, generating surface oxides and hydrogen (H<sub>2</sub>)". Steam activation partially gasifies biochar, facilitating devolatilization and supporting the development of a crystalline structure.<sup>16</sup> Oxygen from water molecules interacts with carbon surface sites, generating surface oxides and hydrogen (H<sub>2</sub>). The generated H<sub>2</sub> then reacts with carbon surface sites, leading to the formation of hydrogen complexes and activation of the biochar surface.<sup>16</sup> For instance, Igalavithana *et al.* investigated the effects of porous texture and surface chemistry on biochars produced from paper mill sludge and pine sawdust *via* slow pyrolysis followed by steam activation.<sup>110</sup> The sludge and pine sawdust were pyrolyzed at 550 °C, yielding biochar with a surface area of 581.7 m<sup>2</sup> g<sup>-1</sup> and pore diameter of 0.4–0.5 nm. Their results showed that the biochar with the highest CO<sub>2</sub> uptake (2.49 mmol g<sup>-1</sup>) and CO<sub>2</sub>/N<sub>2</sub> selectivity (26.7) at 25 °C and 1 bar exhibited the best overall performance for CO<sub>2</sub> capture. Additionally, the presence of high N-surface groups conferred a basic character, which enhanced CO<sub>2</sub> adsorption (Fig. 8).<sup>110</sup> Similarly, Folan *et al.* prepared biochar from cellulose fibers and *Populus nigra* wood using steam-assisted slow pyrolysis for N<sub>2</sub>, CO<sub>2</sub>, and CH<sub>4</sub> capture.<sup>111</sup> The modified biochar displayed a narrow microporous structure with average pore sizes between 0.55 and 0.6 nm. Additionally, increasing the pyrolysis temperature enhanced the micropore volume, enabling CO<sub>2</sub> adsorption between 1.5 and 2.5 mmol g<sup>-1</sup> and CH<sub>4</sub> adsorption between 0.1 and 0.5 mmol g<sup>-1</sup> at room temperature.<sup>111</sup>

To prepare engineered biochar, CO<sub>2</sub> activation is widely implemented in the physical treatments for the fabrication of engineered biochar. Furthermore, CO<sub>2</sub> activation is considered more effective for generating micropores in biochar as compared to steam activation, which are highly desirable for CO<sub>2</sub> adsorption. As a result, CO<sub>2</sub>-activation biochar has significant potential for CO<sub>2</sub> capture under ambient conditions. For example, Gungbenro *et al.* conducted CO<sub>2</sub> activation on date seed biochar, which was carbonized at 800 °C.<sup>112</sup> Activation

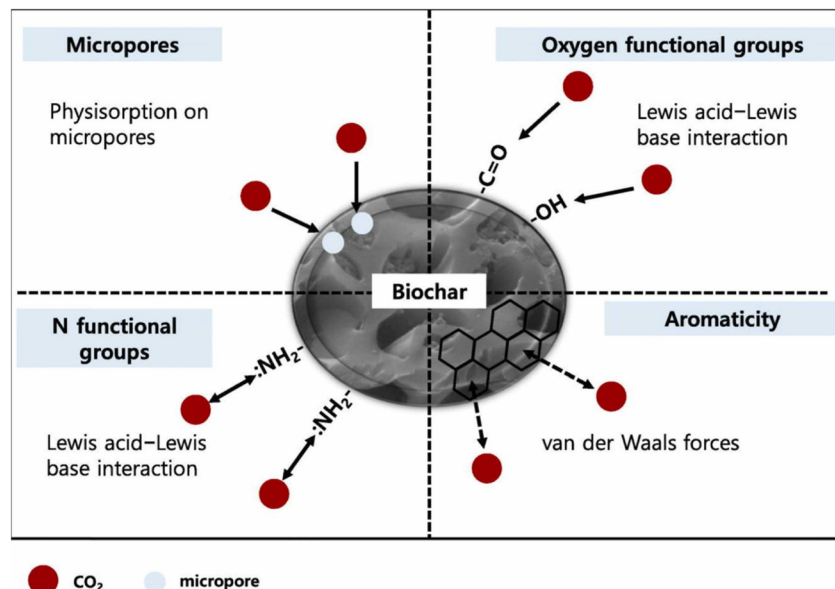


Fig. 8 Simplified scheme of possible mechanisms involved in CO<sub>2</sub> adsorption on biochar. Reproduced with permission from ref. 110. Copyright 2020 Elsevier, B. V.

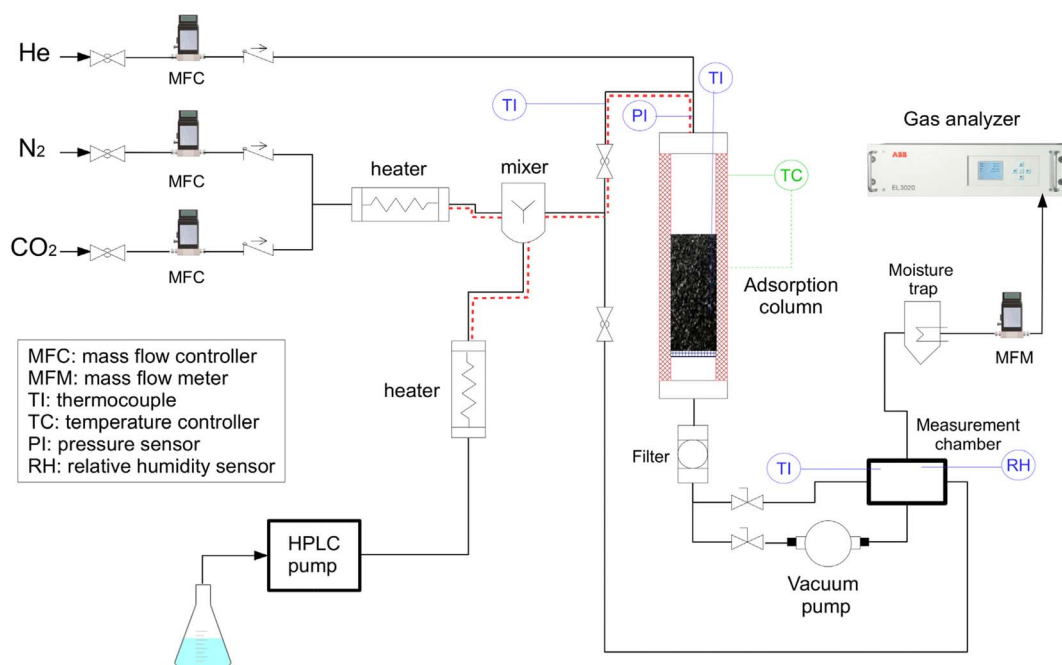


Fig. 9 Schematic diagram of the packed-bed setup used for dynamic breakthrough tests.<sup>113</sup>

under CO<sub>2</sub> at 900 °C for one hour resulted in engineered biochar with a higher CO<sub>2</sub> uptake capacity of 3.21 mmol g<sup>-1</sup> at 20 °C and 2.94 mmol g<sup>-1</sup> at 25 °C, compared to the pristine biochar, which had uptake capacities of 2.07 mmol g<sup>-1</sup> (20 °C) and 1.9 mmol g<sup>-1</sup> (25 °C). This improvement was attributed to the increased micropore volume and BET surface area after CO<sub>2</sub> activation, with values of 0.28 cm<sup>3</sup> g<sup>-1</sup> and 798.38 m<sup>2</sup> g<sup>-1</sup>, respectively—significantly higher than those of the pristine biochar (0.19 cm<sup>3</sup> g<sup>-1</sup> and 531.33 m<sup>2</sup> g<sup>-1</sup>).<sup>112</sup>

A biochar modified by CO<sub>2</sub> activation was also generated from wheat straw and vine shoots.<sup>113</sup> Fig. 9 illustrates a specially designed apparatus used for cyclic adsorption-desorption tests. The prepared biochar exhibited a selective CO<sub>2</sub> physisorption capacity of 1–1.2 mmol g<sup>-1</sup> at 25 °C and 0.14 bar, with an apparent CO<sub>2</sub>/N<sub>2</sub> selectivity of about 50. The biochar's narrow microporosity (49–59%) and uniform ultra-micropore size distribution were key factors in its effectiveness for post-combustion CO<sub>2</sub> capture from dry and wet gas streams.



Table 3 A summary of previous studies on chemical and other modifications of biochar for CO<sub>2</sub> capture

Feedstock	Thermal process	Porosity/surface characteristic-enhancing process	SSA <sup>g</sup> (m <sup>2</sup> g <sup>-1</sup> )	V <sub>t</sub> <sup>b</sup> (cm <sup>3</sup> g <sup>-1</sup> )	V <sub>0</sub> <sup>c</sup> (cm <sup>3</sup> g <sup>-1</sup> )	AFPS <sup>d</sup> (nm)	T (°C)	P (bar)	CO <sub>2</sub> uptake <sup>e</sup> (mmol g <sup>-1</sup> )	(CO <sub>2</sub> /N <sub>2</sub> ) uptake ratio	Reference
<b>Alkaline</b>											
Coconut shells	Carbonization	KOH activation	1172	0.43	0.44	—	25	1	4.23	∞	115
Sargassum & Enteromorpha	Single-step calcination/activation	KOH activation of Sargassum	291.8	0.24	—	—	25	—	1.05	—	116
Bamboo sawdust	Carbonization	KOH activation	540.3	0.22	—	3.85	25	1	3.38	—	117
Bamboo sawdust	Carbonization	KOH activation	728.4	0.29	0.25	2.67	25	—	3.49	25.7	118
Pine wood & sewage sludge	Pyrolysis of 70% pine wood & 30% sewage sludge	KOH activation	2623	0.9	0.74	0.85	25	1	4.14	∞	119
<i>Pinus radiata</i> sawdust	Carbonization	KOH activation	2437	1.09	0.97	—	25	1	3.43	21	120
Pine nut shells	Carbonization	KOH activation	1028	0.57	0.52	<2.2	25	1	3.96	—	155
Pine needles	Slow pyrolysis	KOH activation	1557	0.56	0.62	1.59	25	1	4.05	∞	121
Banana peel waste	Simultaneous carbonization/activation process (KOH & urea impregnation)	KOH activation	2228	0.98	0.73	<2	25	1	3.86	—	122
Chicken manure waste	Fluidised bed pyrolysis	KOH activation	22.22	0.05	—	—	25	1	1.95	—	156
Biowaste (food waste & wood waste)	Gasification of 80% wood waste & 20% food waste	—	294.7	0.05	—	2.3	25	1	~1.75 <sup>a</sup>	—	123
Vine shoots	Slow pyrolysis	KOH activation	1439	0.67	0.49	—	0	1	6.08	—	124
Mesquite wood chips & chicken manure	Gasification of 70% wood chips & 30% chicken manure	KOH activation	1409	0.83	0.36	2.36	25	1	2.92	—	63
Agro-based biomass	700 °C	Miscanthus pyrolysis	532	—	0.21	—	70	0.1 <sup>c</sup>	2.89 <sup>a</sup>	—	157
Agro-based biomass	550–600 °C	Miscanthus pyrolysis	>207	—	0.09	—	70	0.1 <sup>c</sup>	2.53 <sup>a</sup>	—	158
Waste corn straw	Carbonization	Urea-modified corn straw based material/KOH activation	1515	0.75	0.55	—	25	1	4.97	18	147
Sewage sludge & pine sawdust	Slow pyrolysis	KOH activation	2623	0.9	0.68	0.85	25	1	4025	15.85	13

Table 3 (Contd.)

Feedstock	Thermal process	Porosity/surface characteristic-enhancing process	SSA <sup>a</sup> (m <sup>2</sup> g <sup>-1</sup> )	V <sub>t</sub> <sup>b</sup> (cm <sup>3</sup> g <sup>-1</sup> )	V <sub>0</sub> <sup>c</sup> (cm <sup>3</sup> g <sup>-1</sup> )	APS <sup>d</sup> (nm)	T (°C)	P (bar)	CO <sub>2</sub> uptake <sup>e</sup> (mmol g <sup>-1</sup> )	(CO <sub>2</sub> /N <sub>2</sub> ) uptake ratio	Reference
Microalgae (chlorella & spirulina)	Pyrolysis of chlorella	Modification with urea and KOH activation	422.6	0.28	—	2.72	25	1	3.44	34	159
Coffee grounds	Carbonization	KOH activation of melamine-modified biochar	990	0.55	0.45	—	35	1	2.67	∞	135
<b>Amine</b>											
Anaerobic digestate derived from dairy cattle slurry and silage	Slow pyrolysis	Modification with urea	6.89	0.038	—	17.91	25	1	1.22	—	125
Corn stalks	Carbonization	Modification of N-doped-biochar with phytic acid and K <sub>2</sub> CO <sub>3</sub> activation	1136.3	0.39	0.36	—	25	1	3.1	~16	126
Bamboo shoot shell powder	Carbonization	Modification with thiourea	4.08	0.01	0	11.58	25	1	0.5	—	127
Enteromorpha	One-step N/MgO co-doped biochar by microwave induced heating	Modification with thiourea and K <sub>2</sub> CO <sub>3</sub> activation	1454	0.61	0.54	1.68	25	1	3.83	14.3	
Corn cob	Carbonization	Modified using K <sub>3</sub> PO <sub>4</sub>	285.91	—	—	<2	100	1	4.79	79.83	128
Bamboo	Slow pyrolysis	Modification using lignin and microwave irradiation	977	0.48	0.35	<4	25	1	3.8 <sup>a</sup>	1.37–1.64	160
Sewage sludge	Pyrolysis	Conditioning using K <sub>2</sub> FeO <sub>5</sub> and CPAM <sup>1</sup>	340.32	0.233	0.149	—	0	1	3.10	—	71
Medical cotton wool	Carbonization	Modification using DETA <sup>1</sup>	50.92	0.041	—	1.33	50	1	2.15	—	161
Coconut shells	Calcination	KOH activation, urea and surface oxidation with H <sub>2</sub> O <sub>2</sub>	287	—	—	~9	0	1	2.81	≥10	129
Bagasse and hickory chips biomass	Pyrolysis of hickory chips	NH <sub>4</sub> OH doping	563–1495	0.31–0.73	0.25–0.66	1.7–2.2	0	1	5–8	10–30	130
Medical cotton wool	Carbonization	Modification using DETA <sup>1</sup>	584	0.356	0.215	2.6	25	1	1.205 <sup>a</sup>	—	131
			287	—	—	~9	0	1	2.81	≥10	129





Table 3 (Contd.)

Feedstock	Thermal process	Porosity/surface characteristic-enhancing process	SSA <sup>a</sup> (m <sup>2</sup> g <sup>-1</sup> )	V <sub>t</sub> <sup>b</sup> (cm <sup>3</sup> g <sup>-1</sup> )	V <sub>0</sub> <sup>c</sup> (cm <sup>3</sup> g <sup>-1</sup> )	APS <sup>d</sup> (nm)	T (°C)	P (bar)	CO <sub>2</sub> uptake <sup>e</sup> (mmol g <sup>-1</sup> )	(CO <sub>2</sub> /N <sub>2</sub> ) uptake ratio	Reference
Softwood sawmill sawdust	Fast pyrolysis	Activated biochar modification using APTES	394.1	—	0.16	3.08	20	1	3.7 <sup>a</sup>	—	162
Softwood pine biomass	Slow pyrolysis	Activation by EDC <sup>d</sup> and HOBt <sup>e</sup> , then amine TEPA <sup>f</sup> -functionalization	9.39	0.02	0.09	—	70	0.1 <sup>c</sup>	2.79	—	163
<b>Metal &amp; metal oxide</b>											
Walnut shell	Single-step pyrolysis	Impregnation using Mg(NO <sub>3</sub> ) <sub>2</sub> ·6H <sub>2</sub> O	292	0.157	0.118	2.15	30	1	1.82 <sup>a</sup>	—	132
Hickory chips	One-step pyrolysis	Modification using FeCl <sub>3</sub> ·6H <sub>2</sub> O and ball-milling	—	—	—	—	25	1	3.409 <sup>a</sup>	—	133
Rambutan peel	Pyrolysis	Modification by MgO-impregnation	504.6	0.277	0.182	2202	30	1	1.76	∞	134
<b>Other</b>											
Bamboo chips	Fast pyrolysis	Modification using ZIF-8 and carbonization	989.3	0.56	0.39	—	30	1	2.43	—	137
Birch hardwood	Pyrolysis	Modification with MOF—CuBTC	—	—	—	—	25	1	3.7	—	138
Macadamia nut shells	Gasification	Modification with MOF—CuBTC	806.0	0.47	0.33	—	0	1	9.8	>22	140
Rice straw	Fast pyrolysis	Modification with MOF—CuBTC	795.0	0.44	0.34	~2.2	25	1	3.83	>12	141
Leucaena wood	Pyrolysis	Impregnation with ammonium metavanadate	—	—	—	—	30	1	1.2	—	142

<sup>a</sup> Specific surface area: calculated using the BET method. <sup>b</sup> Total pore volume obtained from the amount of N<sub>2</sub> adsorbed at  $p/p_0 \approx 0.95$ . <sup>c</sup> Micropore volume calculated by applying the DR equation to N<sub>2</sub> at -196 °C. <sup>d</sup> Average pore size. <sup>e</sup> Deduced from CO<sub>2</sub> adsorption isotherms.

Additionally, the presence of narrow slit-shaped pores, also referred to as super/ultra-micropores (APS  $\sim 0.7$  nm), can improve the performance mentioned above in the biochar structure, mainly after activation treatment.<sup>113</sup> This has been demonstrated using a palm kernel shell microporous biochar, which achieved a  $\text{CO}_2$  adsorption of  $2.5 \text{ mmol g}^{-1}$  at  $25^\circ\text{C}$  and 1 bar.<sup>109</sup> The presence of specific functional groups on the surface of biochars further enhances  $\text{CO}_2$  capture efficiency. Importantly,  $\text{CO}_2$  activation also promoted the formation of small mesopores in addition to micropores. While micropores enhance  $\text{CO}_2$  adsorption capacity, mesopores facilitate the diffusion of  $\text{CO}_2$  molecules into the biochar pores, improving overall adsorption efficiency.<sup>113,114</sup>

**5.2.2 Chemical modification.** Chemical treatment of biochar can be performed through various methods, including oxidation using basic solutions (*e.g.*, KOH, NaOH, *etc.*), amination by introducing amine functional groups (*e.g.*,  $\text{NH}_3$ ), and impregnation with metal or metal oxide solutions to incorporate basic metals into the biochar structure.<sup>9</sup> Among the chemical modification methods, the most commonly used strategies include alkaline and acid treatments, amination, surfactant modification, and impregnation with metals or metal oxides. These treatments are widely applied to enhance the surface chemistry of biochar. Table 3 provides detailed information on synthesis methodologies, surface area measurements, pore volume data, and sorption characteristics, along with comprehensive examples of modified biochar.

**5.2.2.1 Alkali modification.** Activating biochar by impregnating it with strong bases (KOH), is one of the most efficient methods for enhancing biochar's selectivity and  $\text{CO}_2$  adsorption. The alkalinity of KOH favors the dissolution of acidic  $\text{CO}_2$ , thereby modifying the biochar surface properties.<sup>16</sup> Additionally, potassium species formed during KOH activation diffuse into the internal structure of the biochar, increasing pore width and significantly improving its pore structure. The enhanced

$\text{CO}_2$  adherence to modified biochar surface is primarily achieved by the formation of chemical bonds, predominantly covalent bonds.<sup>15</sup> For example, Yang *et al.* developed biochar from coconut shells *via* carbonization and chemical activation using KOH, achieving a high  $\text{CO}_2$  adsorption capacity of  $4.23 \text{ mmol g}^{-1}$  at  $25^\circ\text{C}$  and 1 bar.<sup>115</sup> The material exhibited a high SSA ( $1172 \text{ m}^2 \text{ g}^{-1}$ ) and a microporous texture (micropore volume,  $V_0 = 0.44 \text{ cm}^3 \text{ g}^{-1}$ ; total pore volume,  $V_t \approx 0.43 \text{ cm}^3 \text{ g}^{-1}$ ). Furthermore, the biochar demonstrated excellent  $\text{CO}_2$  selectivity over  $\text{N}_2$  under the tested conditions. The high adsorption capacity was attributed to the high surface area, well-developed narrow microporosity, and uniform pore size distribution (as indicated by  $V_0 \approx V_t$ ).<sup>115</sup>

Liu and co-author prepared porous biochars from marine algae using a one step KOH-calcination/activation method. The  $\text{CO}_2$  adsorption capacities of the resulting materials were  $0.52$  and  $1.05 \text{ mmol g}^{-1}$  (at  $25^\circ\text{C}$ ) for biochar derived from *Enteromorpha* and *Sargassum* feedstocks, respectively.<sup>116</sup> Their findings demonstrated the crucial role of mass transfer in  $\text{CO}_2$  adsorption.<sup>116</sup> In this regard, enhanced  $\text{CO}_2$  adsorption performance due to increased Lewis basicity, which results in acid-base interactions and selective adsorption, has been reported by Tiwari *et al.* Biochars synthesized from bamboo sawdust by pyrolysis and KOH chemical activation exhibited a notable  $\text{CO}_2$  adsorption capacity of approximately  $3.4 \text{ mmol g}^{-1}$  at  $25^\circ\text{C}$  and 1 bar.<sup>117,118</sup> Fig. 10 depicts the activation process of biochar derived from bamboo. Even higher capacities of up to  $4.14 \text{ mmol g}^{-1}$  were achieved using a biochar mixture composed of 70% pine wood and 30% sewage sludge. This biochar displayed exceptional  $\text{CO}_2/\text{N}_2$  selectivity and retained over 97% regenerability after six consecutive adsorption-desorption cycles.<sup>119</sup> Further research confirmed the efficiency of KOH activation in designing and developing nanoporous biochars with a highly developed surface area ( $2437 \text{ m}^2 \text{ g}^{-1}$ ) and micropore volume above  $0.95 \text{ cm}^3 \text{ g}^{-1}$ .<sup>120</sup> A narrow pore size

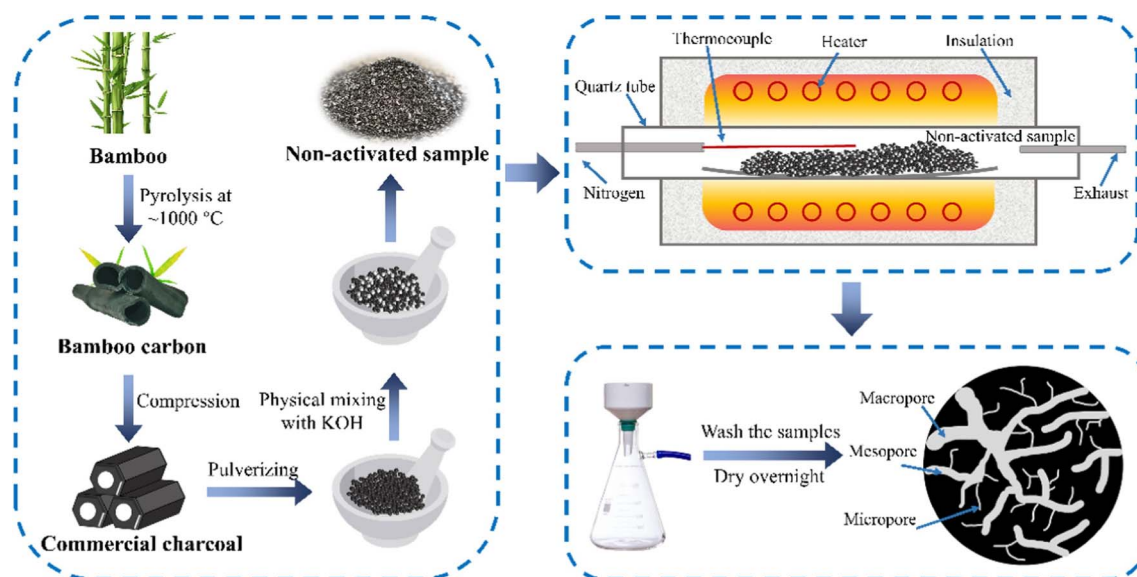


Fig. 10 Schematic diagram for activation of bamboo-derived biochar.<sup>117</sup>



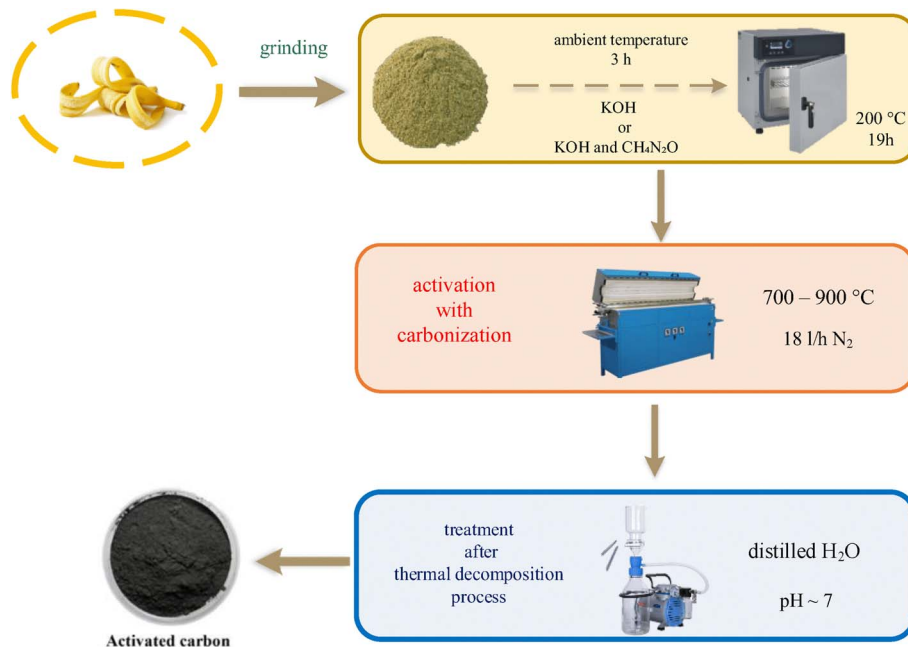


Fig. 11 Schematic illustration for synthesis of banana-derived porous carbons.<sup>122</sup>

distribution, characterized by the absolute dominance of ultramicropores, resulted in CO<sub>2</sub> adsorption capacities above 4 mmol g<sup>-1</sup> at 25 °C and 1 bar.<sup>121</sup> This was evidenced by  $V_0 > V_t$ , indicating diffusional limitations for N<sub>2</sub> adsorption and confirming a narrow micropore size distribution. Additionally, the presence of Ca (54.94% CaO) and N (58.28% N-pyrrolic) species further enhanced the efficiency.<sup>121</sup>

A recent study has reinforced the importance of well-developed ultra-microporosity and a narrow pore size distribution for effective CO<sub>2</sub> capture.<sup>122</sup> For instance, banana peel waste-derived biochar was produced *via* simultaneous carbonization and KOH activation (Fig. 11). The prepared biochar exhibited a high surface area (1623 m<sup>2</sup> g<sup>-1</sup>), a high micropore volume (0.58 cm<sup>3</sup> g<sup>-1</sup>), and a narrow pore size distribution ( $V_t \approx V_0$ ), with an average pore size below 1 nm. This biochar displayed a CO<sub>2</sub> adsorption capacity of 3.74 mmol g<sup>-1</sup> at 25 °C and 1 bar. Moreover, biochar modified using a KOH–urea impregnation route demonstrated even better performance, with a surface area of 2228 m<sup>2</sup> g<sup>-1</sup>, an additional pore volume of 0.31 cm<sup>3</sup> g<sup>-1</sup> and an enhanced microporosity (0.73 cm<sup>3</sup> g<sup>-1</sup>). The slight increase in pore size ( $\pm 1$  nm) due to urea's catalytic role in pore formation improved the CO<sub>2</sub> uptake to  $\sim 3.9$  mmol g<sup>-1</sup> at 25 °C and 1 bar.<sup>122</sup>

Biochar prepared from a 30% sewage sludge and 70% pine sawdust mixture *via* KOH activation demonstrated significantly enhanced textural properties and functional groups compared to pristine counterparts. The microporosity of the modified biochars increased the SSA by 3.9–14.5 times, resulting in CO<sub>2</sub> adsorption capacities of 136.7–182.0 mg g<sup>-1</sup>, compared to only 35.5–42.9 mg g<sup>-1</sup> for the unmodified materials.<sup>119</sup> Xu *et al.* used various activators (KOH, K<sub>2</sub>CO<sub>3</sub>, and ZnCl<sub>2</sub>) to prepare biomass-based porous carbons, revealing that KOH activation yielded

the best pore structure improvement. The SSA increased from 49 m<sup>2</sup> g<sup>-1</sup> to a maximum of 2354 m<sup>2</sup> g<sup>-1</sup>, with a CO<sub>2</sub> adsorption capacity of 3.08 mg g<sup>-1</sup> at 25 °C and 1 bar). Similarly, KOH activation of gasification biochar derived from wood and food waste significantly improved the surface area from 98.9 m<sup>2</sup> g<sup>-1</sup> to 841.3 m<sup>2</sup> g<sup>-1</sup>, confirming KOH's effectiveness as an activator for porous carbons.<sup>123</sup> It was also noticed that KOH acted as an effective activator for the preparation of biochar with porous carbon structures. Additionally, both chemical and physical methods are also used to modify biochar.<sup>124</sup>

**5.2.2.2 Amine modification.** Nitrogen-doped biochar, a green and renewable material, has been used as an alternative to conventional activated biochar for the adsorption of flue gas pollutants, exhibiting enhanced CO<sub>2</sub> adsorption performance. Additionally, functional groups of nitrogen element have been introduced to improve the CO<sub>2</sub> adsorption capacity. The modification of biochar with ammonia or incorporation of basic functional groups, such as N-containing species, increases its affinity for acidic CO<sub>2</sub> enhancing surface alkalinity.<sup>16</sup> Similarly, urea-based modification has been used to convert the digestate from the anaerobic digestion of dairy cattle slurry and silage into N-doped biochar.<sup>125</sup> Textural characterization data indicated that unmodified biochar, obtained *via* slow pyrolysis of the digestate, had an apparent surface area of 13.18 m<sup>2</sup> g<sup>-1</sup> and a total pore volume of 0.047 cm<sup>3</sup> g<sup>-1</sup>. These values decreased further (6.89 m<sup>2</sup> g<sup>-1</sup> and 0.038 cm<sup>3</sup> g<sup>-1</sup>) when the biochar was modified with urea, in line with previously discussed observations regarding potential pore blockage by the used doping agent. However, this modification enhances CO<sub>2</sub> adsorption performance, with urea-modified biochars displaying a CO<sub>2</sub> adsorption capacity of 1.22 mmol g<sup>-1</sup>—higher than that of unmodified biochars (1.0 mmol g<sup>-1</sup>) at 25 °C and 1



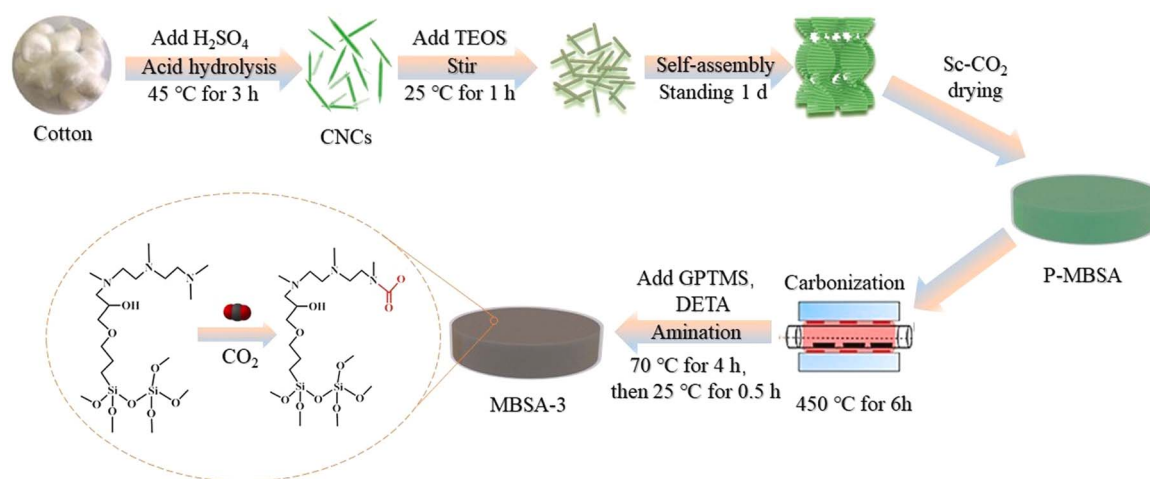


Fig. 12 Flow chart for the preparation of amino-modified biochar-silica hybrid aerogels. Reproduced with permission from ref. 129. Copyright 2020 Elsevier, B. V.

bar. The improvement in adsorption capacity is attributed to the introduction of N-functional groups, despite the relatively underdeveloped porous texture.<sup>125</sup>

Co-doping biochar for CO<sub>2</sub> capture has also been explored.<sup>126–128</sup> For instance, N-doped biochars synthesized *via* the pyrolysis of a melamine-modified cornstalk precursor exhibit an SSA of 608.77 m<sup>2</sup> g<sup>-1</sup>, a total pore volume of 0.23 cm<sup>3</sup> g<sup>-1</sup>, and a micropore volume of 0.07 cm<sup>3</sup> g<sup>-1</sup>. These materials demonstrated a CO<sub>2</sub> adsorption capacity of 1.1 mmol g<sup>-1</sup> at 25 °C and 1 bar.<sup>126</sup> Further modification using phytic acid (C<sub>6</sub>H<sub>18</sub>O<sub>24</sub>P<sub>6</sub>) as a phosphorus source and potassium carbonate (K<sub>2</sub>CO<sub>3</sub>) as an activating agent resulted in N and P-co-doped biochars, which exhibited an increased CO<sub>2</sub> adsorption capacity of 3.1 mmol g<sup>-1</sup>, with a CO<sub>2</sub>/N<sub>2</sub> selectivity of about 16. The observed performance could be associated with a multi-action synergy, *i.e.*, the action of N-groups beneficial for CO<sub>2</sub> capture as well as the dual action of phosphorus acting as an activating agent (SSA = 1136.31 m<sup>2</sup> g<sup>-1</sup>) corroding the carbon skeleton at high temperatures to form porous layered structures and leading to a narrow pore size distribution ( $V_t \approx V_0$ ), and as a heteroatomic doping source culminating in enhanced CO<sub>2</sub> chemisorption.<sup>126</sup> Similarly, the synergistic effect between the microporous texture (ultra-micropores, narrow micropore size distribution, *etc.*) and the presence of heteroatoms in CO<sub>2</sub> capture has been demonstrated in N, S-doped biochars derived from bamboo shoot shells, using thiourea as a dual-source of N and S, and K<sub>2</sub>CO<sub>3</sub> as an activating agent.<sup>127</sup> The N, S-co-doped biochar, with an SSA of 1454.11 m<sup>2</sup> g<sup>-1</sup>, exhibited a CO<sub>2</sub> adsorption of 4 mmol g<sup>-1</sup>, with a CO<sub>2</sub>/N<sub>2</sub> selectivity above 14. In another study, MgO-loaded N-rich porous biochar was developed from marine biomass (*Enteromorpha*) using single-step microwave-induced heating.<sup>128</sup> This biochar (SSA = 285.9 m<sup>2</sup> g<sup>-1</sup>) was designed for selective CO<sub>2</sub> adsorption and demonstrated excellent performance, with a CO<sub>2</sub>/N<sub>2</sub> ratio of 79.83 and an adsorption capacity of 4.79 mmol g<sup>-1</sup> at 100 °C and 1 bar). The enhanced performance is attributed to the material's microporous nature and the abundance of basic sites, further

facilitated by microwave-induced heating, which promoted a gradual porous structure formation. Additionally, the presence of alkaline N-containing species and the incorporation of MgO nanoparticles further improved CO<sub>2</sub> adsorption performance.<sup>128</sup>

Recent studies have also explored novel biochar designs.<sup>129</sup> For instance, amino-modified biochar-silica hybrid aerogels were prepared from medical cotton wool, carbonized, and post-modified using diethylenetriamine (DETA) for CO<sub>2</sub> capture applications (Fig. 12). These hybrid biochars showed a CO<sub>2</sub> adsorption capacity of 2.81 mmol g<sup>-1</sup> at 0 °C and 1 bar, along with a CO<sub>2</sub>/N<sub>2</sub> selectivity greater than 10. Textural characterization revealed an SSA of 287 m<sup>2</sup> g<sup>-1</sup>, indicating N<sub>2</sub> multilayer adsorption on mesoporous materials. Despite the absence of micropores, selective CO<sub>2</sub> adsorption was correlated with the surface loading DETA, demonstrating an improved CO<sub>2</sub> capture performance.<sup>129</sup> The nitrogen-doped biochar (TF) has also been investigated for its surface functional group (SFG) effect on CO<sub>2</sub> adsorption properties.<sup>130</sup> This biochar was produced *via* calcination of coconut shell with molten alkali KOH as an activator and urea as a nitrogen source (Fig. 13A and B). Further oxidation with H<sub>2</sub>O<sub>2</sub> solutions of varying concentrations (1–15%) yielded modified porous biochars (OTFs). Among them, OTF-10 demonstrated higher adsorption and CO<sub>2</sub>/N<sub>2</sub> selectivity at 273 K. Additionally, OTF-modified biochar exhibited higher dynamic adsorption capacity and extended breakthrough time when exposed to a mixture of CO<sub>2</sub> and N<sub>2</sub> gases (molar ratio 15 : 85) at both 273 K and 298 K.<sup>130</sup> In another study, Xu *et al.* fabricated N-doped biochar *via* NH<sub>4</sub>OH ball milling, incorporating amine (–NH<sub>2</sub>) and nitrile (–C≡N) functional groups onto the biochar surface.<sup>131</sup> The N-doped biochar material exhibited a 31.6–55.2% increase in CO<sub>2</sub> adsorption capacity compared to pristine biochar, attributed to the strong dipole–dipole interactions between the CO<sub>2</sub> molecule's large quadrupole moment and the N-associated polar sites.<sup>131</sup>

**5.2.2.3 Metal and metal oxide modified biochar.** Several studies have explored the use of metal oxyhydroxide biochar



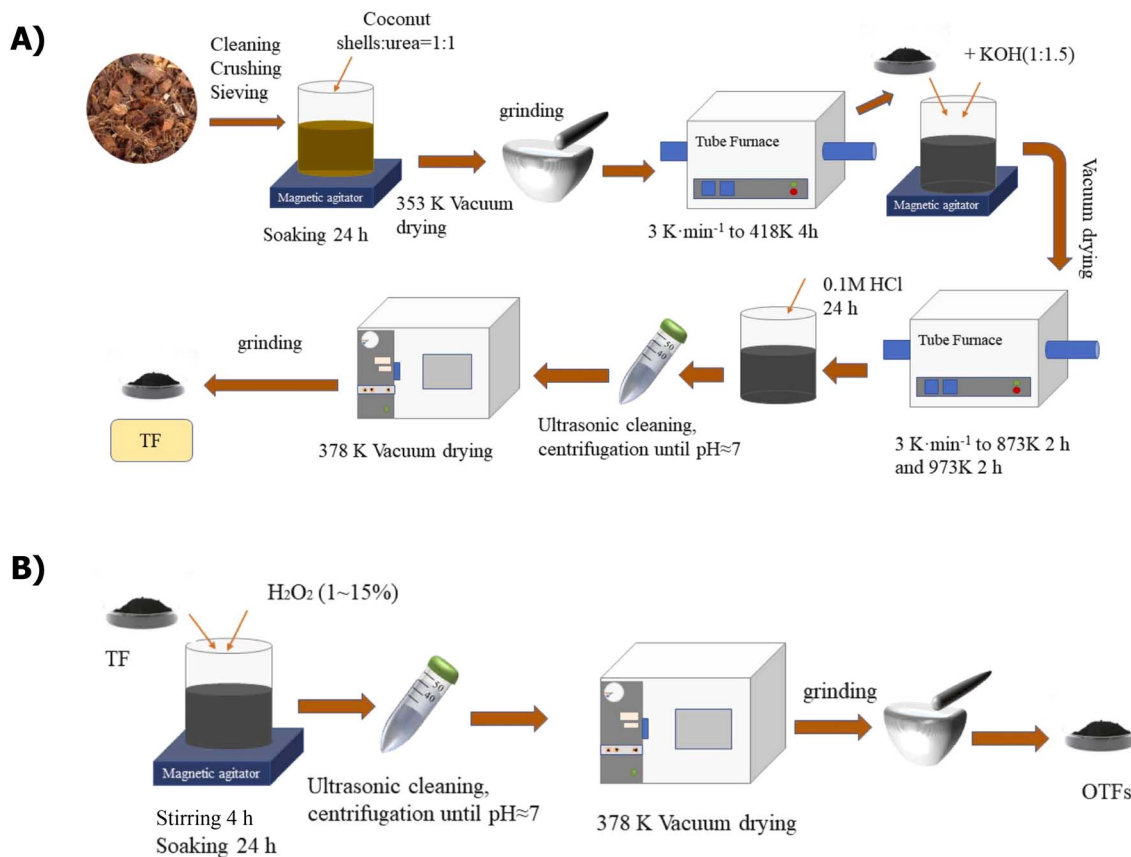


Fig. 13 (A) preparation of nitrogen doped biochar TF and (B) surface oxidation modification of TFs. Reproduced with permission from ref. 130. Copyright 2023 Elsevier, B. V.

composites for effective capturing of CO<sub>2</sub> by biochar. It has been observed that increasing the alkalinity of the biochar surface can improve the adsorption of acidic CO<sub>2</sub>. Therefore, introducing metal groups such as Na, Al, Ca, Ni, Mg, and Fe onto the biochar surface increases the number of basic sites, making this approach a promising strategy for improving CO<sub>2</sub> adsorption capacity.<sup>132</sup>

$$n_{\text{ads}_{\text{biochar}}} < n_{\text{ads}_{\text{biochar-Ca}}} < n_{\text{ads}_{\text{biochar-Ni}}} < n_{\text{ads}_{\text{biochar-Fe}}} < n_{\text{ads}_{\text{biochar-Al}}} < n_{\text{ads}_{\text{biochar-Mg}}}$$

Metal incorporation has generally enhanced the performance of biochar for targeted application. The textural characterization of both pristine biochar and Mg-biochar revealed a decrease in surface area ( $\pm 100 \text{ m}^2 \text{ g}^{-1}$ ) and total pore/micropore volume ( $\pm 0.04 \text{ cm}^3 \text{ g}^{-1}$ ) due to the presence of metallic magnesium. The observed improvement in CO<sub>2</sub> adsorption capacity can be attributed to a synergistic effect between the physisorption mechanism and chemical interactions between the basic MgO groups and the acidic CO<sub>2</sub> molecules.<sup>132</sup> Biochars have also been synthesized from hickory chips (HC) using a one-step pyrolysis process.<sup>133</sup> In parallel, Fe oxyhydroxide-biochar composites have been modified using FeCl<sub>3</sub>·6H<sub>2</sub>O, followed by single-step pyrolysis or an additional

ball-milling step.<sup>131</sup> The CO<sub>2</sub> capture performance of the biochar was evaluated, showing an increase in adsorption capacity at 25 °C and 1 bar. The ball-milled Fe-oxyhydroxide-biochar composite adsorbed approximately  $3.4 \text{ mmol CO}_2 \text{ g}^{-1}$ , compared to  $2.95 \text{ mmol g}^{-1}$  for the non-ball-milled counterpart and  $1.093 \text{ mmol g}^{-1}$  for unmodified HC biochar. This enhancement was initially attributed to physisorption but transitioned to chemical interaction between Fe oxyhydroxide and CO<sub>2</sub> with increasing Fe-content in the composite.<sup>133</sup> Other metal oxide-biochar composites have been prepared by modifying biochar derived from *Nephelium lappaceum* (rambutan) peel pyrolysis with a magnesium salt *via* impregnation.<sup>134</sup> The textural characterization confirmed that these materials exhibited well developed porosity ( $\sim 600 \text{ m}^2 \text{ g}^{-1}$  for pristine biochar and  $\sim 505 \text{ m}^2 \text{ g}^{-1}$  for the modified biochar), with a total pore volume of  $0.31 \text{ cm}^3 \text{ g}^{-1}$  and  $0.28 \text{ cm}^3 \text{ g}^{-1}$ , and a micropore volume of  $0.2 \text{ cm}^3 \text{ g}^{-1}$  and  $0.18 \text{ cm}^3 \text{ g}^{-1}$ , respectively. The modification process reduced the available porosity, yet metal oxide-biochar composites demonstrated superior CO<sub>2</sub> adsorption at 30 °C and 1 bar compared to unmodified biochars. While metal incorporation blocked some micropore openings, chemical interaction between MgO and CO<sub>2</sub> significantly enhanced capture capacity. The CO<sub>2</sub> adsorption capacity of metallized biochar ( $76.80 \text{ mg g}^{-1}$ ) was notably higher than that of pristine biochar ( $68.74 \text{ mg g}^{-1}$ ), which can be attributed to the



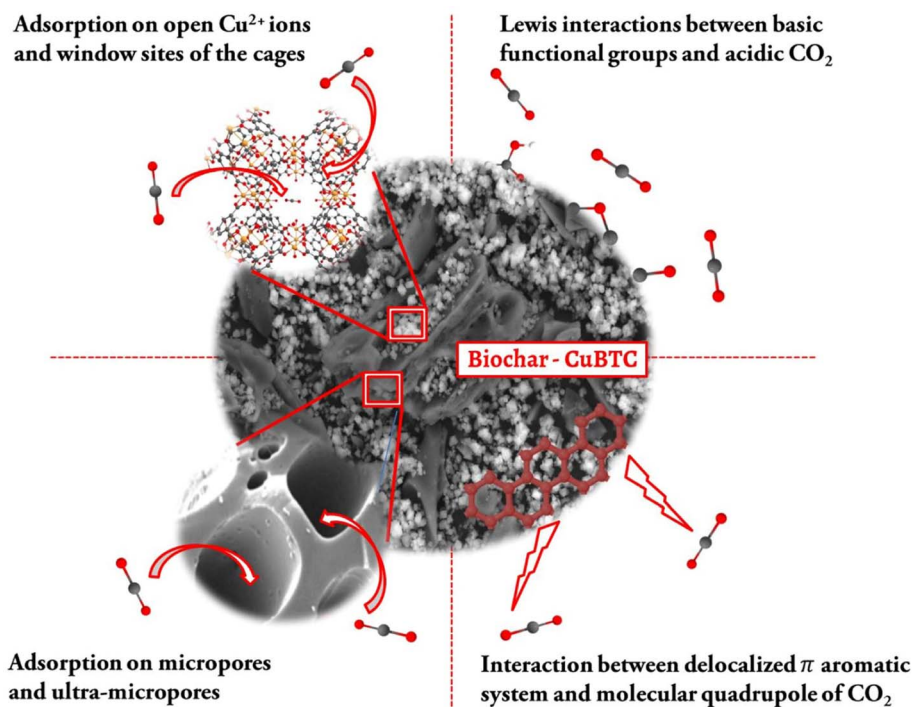


Fig. 14 CO<sub>2</sub> adsorption mechanisms of biochar-CuBTC composites.<sup>140</sup>

combined influences of physicochemical characteristics. Furthermore, this study demonstrated that the metallized biochar maintained stable adsorption performance over 25 cycles of CO<sub>2</sub> adsorption-desorption.<sup>134</sup> Biochars have also been prepared from walnut shells *via* one-step pyrolysis at different temperatures (500, 700, and 900 °C) under a N<sub>2</sub> atmosphere.<sup>132</sup> The as-fabricated biochar at high temperature (900 °C) exhibited a SSA of 397.015 m<sup>2</sup> g<sup>-1</sup> and microporosity of 0.159 cm<sup>3</sup> g<sup>-1</sup>. To incorporate metal components into biochar, metal impregnation was performed by thermal treatment with N<sub>2</sub>. In this, various metal nitrate salts (NaNO<sub>3</sub>, Ca(NO<sub>3</sub>)<sub>2</sub>, Mg(NO<sub>3</sub>)<sub>2</sub>, Al<sub>2</sub>(NO<sub>3</sub>)<sub>3</sub>, Ni(NO<sub>3</sub>)<sub>2</sub> and Fe<sub>2</sub>(NO<sub>3</sub>)<sub>3</sub>) were impregnated into biochar *via* thermal treatment under N<sub>2</sub>. Results indicated that adding basic sites *via* metal impregnation improved CO<sub>2</sub> capture. The order of CO<sub>2</sub> adsorption efficiency of the above metal impregnated biochar is as follows; Mg<sup>2+</sup> > Al<sup>3+</sup> > Fe<sup>3+</sup> > Ni<sup>2+</sup> > Ca<sup>2+</sup> > unmodified biochar > Na<sup>+</sup>. Mg<sup>2+</sup>-loaded biochar displayed the highest CO<sub>2</sub> uptake (82.0 mg g<sup>-1</sup>), surpassing pristine biochar (72.6 mg g<sup>-1</sup>) at 25 °C and 1 atm, due to the combined effects of physical and chemical interaction.<sup>132</sup> Likewise, walnut shell biochars were modified by incorporating various metals *via* simple impregnation, followed by heat treatment to enhance CO<sub>2</sub> adsorption capacity.<sup>135</sup> Among these, Mg-loaded biochar demonstrated the highest CO<sub>2</sub> capture capacity (80.0 mg g<sup>-1</sup>) compared to raw biochar (69.1 mg g<sup>-1</sup>).<sup>132</sup>

**5.2.2.4 Other modifications.** Integration of nanomaterials into highly porous, surface-active, and structurally stable biochar results in innovative nanocomposites that leverage the well-established benefits of both materials. Additionally, biochar-MOF composites were prepared from walnut shell-

feedstock using a sol-gel modification route followed by pyrolysis.<sup>136</sup> Briefly, the modified biochar, BC/Mg-MOF-74, was prepared *via* an *in situ* growth method and subsequently tested for CO<sub>2</sub> capture. During CO<sub>2</sub> adsorption on Mg-MOF-74-modified biochar, chemical bonds were formed, as evidenced by the adsorption energy value (below -42 kJ mmol<sup>-1</sup>), indicating the dominance of the chemisorption mechanism.<sup>136</sup>

As part of the zeolite imidazole framework (ZIF) series, one of the zeolitic imidazolate ZIF-8 possesses well-ordered nitrogen groups and a porous structure. Furthermore, it undergoes pore structure reconstruction and nitrogen group transformation during heat treatment. These characteristics enable ZIF-8 to modify or be compounded with other materials to enhance adsorption performance. An uncomplicated, activation-free method for synthesizing nitrogen-doped porous materials was developed by co-carbonizing biochar with ZIF-8.<sup>137</sup> Thermal treatment with ZIF-8 enhanced the porosity of the resulting materials, especially their microporosity, with the effect becoming more significant at higher carbonization temperatures. Interestingly, the surface area of biochar was increased dramatically from 3.0 to 989.3 m<sup>2</sup> g<sup>-1</sup>, while its CO<sub>2</sub> adsorption capacity improved from 0.52 to 2.43 mmol g<sup>-1</sup> (1 atm, 30 °C) after modification. Additionally, ZIF-8 grafting and annealing enhanced the vdW interactions between biochar and CO<sub>2</sub> molecules, leading to a 260% increase in CO<sub>2</sub> adsorption capacity.<sup>137</sup>

A previous study demonstrated that incorporation of biochar into copper benzene-1,3,5-tricarboxylate (CuBTC) composites, with biochar content ranging from 5% to 30%, notably enhanced CO<sub>2</sub> uptake—reaching up to 3.7 mmol g<sup>-1</sup> at 1 bar



and 25 °C—compared to the original materials. The composite also exhibited good stability over 20 adsorption–desorption cycles.<sup>138</sup> Moreover, the CuBTC-biochar composite significantly improved CuBTC's moisture resistance, a critical limitation of CuBTC alone.<sup>139</sup> In another study, a cost-effective nanocomposite was fabricated through an electrochemical approach, combining CuBTC with the low-cost post-gasification residue of macadamia nut shells.<sup>140</sup> The CO<sub>2</sub> adsorption mechanisms of biochar-CuBTC composites is illustrated in Fig. 14. Likewise, this study provided valuable insight into the potential of hydrochar and CuBTC composites as potential CO<sub>2</sub> adsorption materials.<sup>141</sup> Additionally, studies have explored other biochar-based composites for CO<sub>2</sub> capture. For example, biochar derived from woody biomass, modified with vanadium oxide, has been studied as a potential CO<sub>2</sub> adsorbent.<sup>142</sup> Similarly, activated magnesium oxide nanoparticles produced from biomass have shown remarkable CO<sub>2</sub> capture capacity.<sup>143</sup> Furthermore, Ag/MgO/biochar nanocomposites were prepared employing solvent-free ball milling methods.<sup>144</sup>

## 6 Performance and comparison of biochar and biochar-based materials in CO<sub>2</sub> capture

A broad variety of biochar and biochar-based materials have been fabricated to capture CO<sub>2</sub> from the atmosphere. Until now, various biochar materials have been produced using different raw materials, modifications, and synthetic approaches. A thorough performance assessment was conducted by comparing biochar and biochar-based materials derived from various raw materials and preparation methods, with emphasis on adsorption capacity, selectivity, and reusability (Tables 1–3). After such comparative evaluation, the preferred raw materials, modification strategies, and modification types for capturing CO<sub>2</sub> from the atmosphere can be easily selected.

It is important to note that the performance data summarized in Tables 1–3 are primarily measured under dry conditions. In practical DAC applications, atmospheric moisture is a ubiquitous and competing adsorbate that can significantly alter the performance. The presence of humidity can lead to competitive adsorption on polar sites, pore blockage *via* water condensation, and for some materials, promote hydrolytic instability. While some chemically modified biochars (*e.g.*, amine-impregnated) may show enhanced affinity for CO<sub>2</sub> in moist streams due to different adsorption mechanisms, others (especially purely microporous, physically activated biochars) often experience capacity reduction. Therefore, the optimal material selection must consider this critical variable. The brief mentions of “wet conditions” in the review highlight this complexity but underscore the need for future standardized reporting to include performance metrics under controlled humidity levels.

Adsorption capacity is a key factor in the effectiveness of biochar and biochar-based materials for capturing CO<sub>2</sub> from the atmosphere. For pristine biochar, the highest adsorption capacity was recorded for biochar derived from date leaves

pyrolyzed at different temperatures.<sup>96</sup> This pristine biochar was prepared at 300, 400, 500, and 600 °C, and its CO<sub>2</sub> adsorption capacity increased from 2.045 to 5.682 mmol g<sup>-1</sup> as the pyrolysis temperature rose. This trend suggests that higher pyrolysis temperatures improved the carbon content of biochar, thereby enhancing its CO<sub>2</sub> capture performance.<sup>96</sup> The second-highest adsorption capacity was observed in lignin-based biochar, produced from high-ash-content (~46%) alkali lignin by pyrolyzing it at 750 °C in a muffle furnace for 3 hours. This biochar demonstrated a peak CO<sub>2</sub> adsorption capacity of 4.06 mmol g<sup>-1</sup> at 0 °C, with an SSA of 1134 m<sup>2</sup> g<sup>-1</sup>, a micropore volume of 0.49 cm<sup>3</sup> g<sup>-1</sup> and total pore volume of 0.84 cm<sup>3</sup> g<sup>-1</sup>.<sup>145</sup> The third-highest CO<sub>2</sub> adsorption capacity was achieved by lignin-based biochar synthesized under negative pressure during pyrolysis. The effect of pressure on the carbonization of high-ash-content alkali lignin at 800 °C for 3 hours was investigated. They found that lower pressure during pyrolysis enhanced CO<sub>2</sub> adsorption capacity, micropore volume and SSA while reducing carbon yield. The optimized biochar, produced under negative pressure (–0.1 MPa), exhibited a SSA of 1577 m<sup>2</sup> g<sup>-1</sup>, a micropore volume of 0.695 cm<sup>3</sup> g<sup>-1</sup>, and a CO<sub>2</sub> adsorption capacity of ~3.6 mmol g<sup>-1</sup> at 0 °C.<sup>144</sup>

For physically modified biochar, a rice husk-derived biochar prepared through physical modification, with an SBET of 1097 m<sup>2</sup> g<sup>-1</sup>, achieved the best adsorption capacity of 3.1 mmol g<sup>-1</sup> at 1 bar and 0 °C.<sup>146</sup> The second highest adsorption capacity was obtained by biochar synthesized through pyrolysis in a furnace, followed by activation in CO<sub>2</sub> at different temperatures (600–900 °C). The biochar modified at 800 °C and activated at 900 °C for 1 hour displayed the highest CO<sub>2</sub> adsorption capacity, reaching 2.94 mmol g<sup>-1</sup>, which is due to the superior textural properties (a micropore volume of 0.28 cm<sup>3</sup> g<sup>-1</sup>, a micropore area of 712.87 m<sup>2</sup> g<sup>-1</sup> and a BET SSA of 798.38 m<sup>2</sup> g<sup>-1</sup>).<sup>112</sup> The CO<sub>2</sub>-activated biochar derived from palm kernel shell for CO<sub>2</sub> capture also achieved good adsorption capacity. The authors investigated various parameters such as CO<sub>2</sub> flow rate (150–450 mL min<sup>-1</sup>), holding time (60–120 min) and activation temperature (750–950 °C) for the fabrication of engineered biochar. The best adsorption performance was achieved at 950 °C (activation temperature), 60 min (holding time), and 150 mL min<sup>-1</sup> CO<sub>2</sub> flow rate, yielding 61.37 wt% of the product with a CO<sub>2</sub> uptake capacity of 2.49 mmol g<sup>-1</sup>.<sup>109</sup>

In this case of chemical modification, the impregnation of 3% vanadium salt into LW-derived biochar exhibited the highest CO<sub>2</sub> adsorption capacity of 9.8 mmol g<sup>-1</sup>, which is due to the oxygen vacancy of vanadium oxide and highly microporous structure of the prepared biochar, resulting in the capture of CO<sub>2</sub> *via* chemisorption. In addition, vanadium salt impregnated biochar (LW900) showed remarkable performance in the capture of CO<sub>2</sub> gas with high selectivity over other gases (N<sub>2</sub>, CH<sub>4</sub>, and air). Importantly, the adsorbent demonstrated excellent regenerability, as it was fully regenerated in 15 min at 110 °C and maintained stable adsorption capacity over 11 consecutive adsorption–desorption cycles with almost no loss of efficiency, indicating that the prepared biochar exhibits good stability and low-energy regeneration potential.<sup>142</sup> This type of chemisorbent may exhibit different interactions with humid



streams compared to physisorbents, though its stability under such conditions requires separate validation. The vine shoot-derived biochar modified physically and chemically with KOH achieved the second higher CO<sub>2</sub> adsorption capacity of 6.08 mmol g<sup>-1</sup> at 25 °C.<sup>124</sup> Furthermore, engineered biochar was fabricated from corn straw using triethanolamine and ethylenediamine as modifiers at 25 °C and 1 bar, achieving a higher CO<sub>2</sub> adsorption capacity of 4.97 mmol g<sup>-1</sup>.<sup>147</sup> These amine-functionalized materials are particularly relevant for humid conditions, as the amine groups can react with CO<sub>2</sub> even in the presence of water, though competitive adsorption and oxidative stability remain key considerations.

## 7 Biochar for CO<sub>2</sub> capture: challenges and future perspectives

Biochar is increasingly recognized as a promising adsorbent for selectively capturing CO<sub>2</sub> from post-combustion emissions. Its attractiveness stems from its versatile porous structure, often characterized by well-developed microporosity and narrow pore size distribution (for example, chemically activated biochar with KOH),<sup>115,122</sup> as well as its highly tunable surface chemistry, which can be modified through heteroatom co-doping (for example, N and S).<sup>127</sup> Despite these advantages, the large-scale implementation of biochar as a CO<sub>2</sub> adsorbent remains constrained by several technical and economic challenges. To provide a clearer overview, Fig. 15 presents a schematic summary of the key issues, including synthesis feasibility, cost considerations, performance under realistic operating conditions, regeneration efficiency, and integration into treatment systems.

Although biochar generally exhibits high surface area, its CO<sub>2</sub> uptake is typically lower than that of benchmark adsorbents such as activated carbons, MOFs, or carbon molecular sieves.<sup>110</sup> While targeted modifications, such as nitrogen doping or steam activation, can enhance adsorption performance, the

variability in biochar properties due to biomass type and pyrolysis conditions complicates standardization for industrial-scale applications. Incorporating nitrogen-containing groups such as amines or imidazoles has been shown to significantly increase CO<sub>2</sub> affinity, but the high cost and limited sustainability of nitrogenating agents (*e.g.*, urea, ammonia, and melamine) hinder scalability and raise concerns regarding economic feasibility.<sup>135,137</sup> Moreover, most studies are conducted under controlled laboratory conditions ( $\leq 1$  bar,  $\leq 70$  °C), which do not reflect the fluctuating temperatures, pressures, and multicomponent gas mixtures (H<sub>2</sub>O, O<sub>2</sub>, NO<sub>x</sub>, and SO<sub>x</sub>) encountered in real flue gases. These factors may reduce adsorption efficiency and compromise long-term stability. Another major limitation lies in regeneration, since industrial viability requires adsorbents that can be regenerated efficiently with minimal energy input. While physisorption-based mechanisms allow for easier regeneration, chemical modifications that promote stronger CO<sub>2</sub> binding often reduce recyclability, and repeated adsorption-desorption cycles generally lead to progressive loss of performance. Finally, successful industrial application requires biochar to be engineered in practical formats such as pellets, granules, foams, or membranes, optimized for use in adsorption columns and fluidized systems to ensure both compatibility and high efficiency.

A critical yet under reported barrier is the economic viability at scale. While lab-scale biochar production from waste biomass can be low-cost (~\$50–500 per tonne for pristine biochar), the costs escalate significantly for engineered variants. Chemical activation, doping with expensive agents (*e.g.*, ionic liquids, specific metal precursors), and multi-step modifications can increase production costs to an estimated \$1000–5000 per tonne, rivaling or exceeding the cost of commercial zeolites or activated carbons.<sup>148–150</sup> Projections for industrial-scale production suggest that economies of scale could reduce these costs by 30–60%, but achieving this requires continuous, high-throughput processing systems not yet demonstrated for

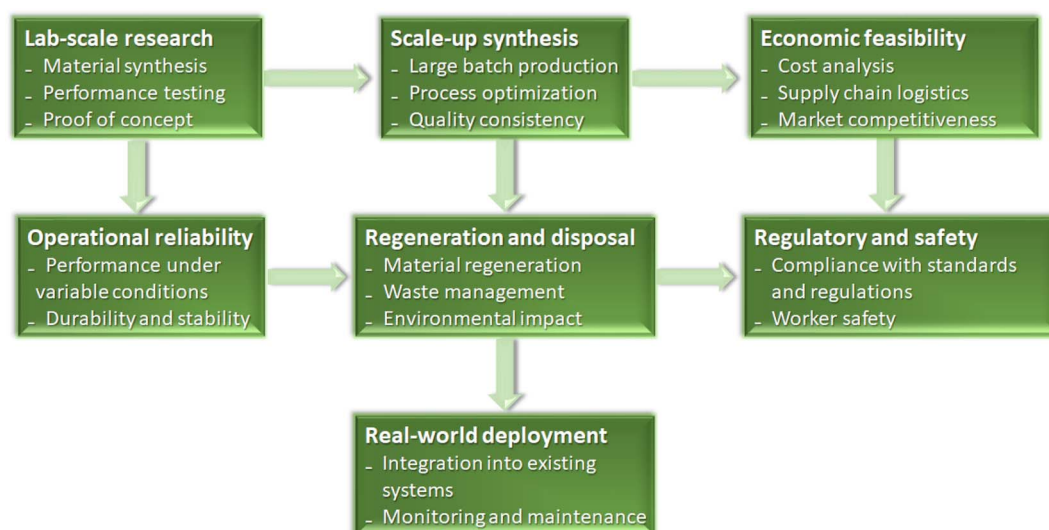


Fig. 15 Scalability and deployment challenges of biochar-based CO<sub>2</sub> adsorption systems.



complex engineered biochars. Furthermore, a comprehensive cost breakdown—encompassing feedstock pre-treatment, activation, shaping, and regeneration energy—is rarely available, highlighting a major gap in the techno-economic analysis literature for biochar-based CO<sub>2</sub> capture systems.

Directly related to the manuscript's title, the transition "From Lab to Industrial Scale Applications" faces substantial hurdles beyond cost. A significant barrier is the lack of standardized, scalable protocols for producing consistent engineered biochar with uniform properties (pore structure, surface chemistry, mechanical strength) in tonnage quantities. Scaling up chemical modification processes (*e.g.*, impregnation, functionalization) introduces challenges in mixing efficiency, heat and mass transfer, and waste stream management not encountered in batch lab reactors. Moreover, shaping biochar powder into robust, low-pressure-drop pellets or monoliths suitable for packed-bed or fluidized-bed reactors without compromising adsorption capacity remains an engineering challenge. Crucially, there is a notable absence of published industrial partnership case studies or commercial deployment data specifically for biochar in CO<sub>2</sub> capture, which limits the understanding of long-term performance in real flue gas streams, operational maintenance issues, and full-system integration costs. Future work must prioritize pilot-scale demonstrations in partnership with industry to generate these essential data.

It is also pertinent to acknowledge that direct CO<sub>2</sub> adsorption represents only one pathway within a broader carbon capture and utilization landscape. A complementary and industrially adopted method is the accelerated carbonation curing of cementitious materials, where biochar is incorporated to enhance CO<sub>2</sub> mineralization. In this process, biochar acts as a nucleation site and pH modifier, facilitating the reaction of CO<sub>2</sub> with calcium silicates to form stable carbonates, thereby permanently sequestering carbon while potentially improving the mechanical properties and durability of the construction material.<sup>151–153</sup> This application highlights biochar's versatility and underscores the importance of developing multi-functional materials for different carbon capture scenarios.

To overcome these barriers, future research should focus on several complementary strategies. Optimizing pyrolysis conditions and carefully selecting biomass feedstocks are essential to produce biochars with high microporosity, homogeneous pore size distribution, and tailored surface functionalities. Developing hybrid and composite materials by integrating biochar with advanced adsorbents such as MOFs, polymers, or metallic nanoparticles offers another promising pathway to enhance adsorption performance, regeneration efficiency, and structural stability. In parallel, emerging modification approaches, including ultrasonic treatment, plasma functionalization, and electrochemical activation, provide opportunities to engineer biochar surfaces with high precision while reducing environmental and economic costs. The establishment of robust predictive models that link feedstock characteristics, processing parameters, and material properties will be critical to improving design reproducibility, scalability, and process control. Furthermore, comprehensive environmental

evaluations, including life cycle assessments, should accompany technological advances to ensure that biochar deployment contributes positively to carbon mitigation without unintended ecological burdens. Most critically, the field must move decisively beyond laboratory-scale research. Prioritizing pilot- and industrial-scale demonstrations under realistic flue gas conditions, coupled with transparent techno-economic analyses and life cycle assessments, is imperative. These studies will provide the essential data on long-term efficiency, stability, system integration, and true cost-effectiveness needed to attract commercial investment and guide policy support.

In summary, advancing biochar for CO<sub>2</sub> capture requires a dual approach: improving adsorption efficiency and regenerability through innovative synthesis and modification methods, while simultaneously validating these improvements under real operating conditions with rigorous sustainability and economic assessments. A holistic view that considers both direct adsorption and indirect utilization pathways, such as carbonation curing, will be crucial. For biochar to fulfill its promise as a scalable industrial adsorbent, future efforts must explicitly bridge the "lab-to-industry" gap by addressing the economic and engineering scalability challenges outlined here. If these challenges are systematically addressed, biochar has the potential to emerge as a scalable, cost-effective, and environmentally sustainable material, capable of playing a significant role in global efforts to mitigate climate change.

## 8 Conclusions

In this work, we have discussed different methods for producing biochar and biochar-based materials, highlighting their advantages and disadvantages. Due to their strong affinity and high selectivity, biochar and its derivatives show great potential for CO<sub>2</sub> capture. They have proven to be effective adsorbents for selectively capturing CO<sub>2</sub>. Activation with different chemicals and nanomaterials can improve the selectivity of biochar materials and potentially enhance their performance, such as increasing their adsorption capacity. Among the methods reported, biochar modified with vanadium oxide exhibited the most impressive performance, with a CO<sub>2</sub> binding capacity of 9.8 mmol g<sup>-1</sup>, excellent stability (11 cycles of CO<sub>2</sub> adsorption–desorption with almost no loss of efficiency), and good selectivity in the presence of other gases (*e.g.*, air, CH<sub>4</sub>, and N<sub>2</sub>). The synthesized biochar-based materials exhibited exceptional CO<sub>2</sub> separation performance, with high selectivity attributed to vanadium oxide, which functioned as an oxygen defect or vacancy species on the surface of 3% V-LW900, facilitating interaction with CO<sub>2</sub> oxygen species.

Despite the effectiveness of biochar and biochar-based materials for CO<sub>2</sub> removal, several challenges remain, such as complex synthesis routes, the use of multiple reagents, extended reaction times, and the need for specific ligand chemistry. These factors limit their broader application in CO<sub>2</sub> capture technologies. Importantly, further research is required on the regeneration of biochar and biochar-based materials to improve their long-term feasibility for CO<sub>2</sub> removal.



Additionally, real-world application studies should be conducted to assess the practical use of these materials.

A rational approach to the production and utilization of novel biochar and biochar-based materials is crucial to meet three key criteria for selective CO<sub>2</sub> removal: outstanding CO<sub>2</sub> selectivity, high adsorption capacity, and stable performance. Current synthesis methods are still in the early stages and need further optimization to become more effective. Furthermore, synthesis time should be carefully considered as a key factor in optimizing energy, resources, and efficiency. There is also significant potential for integrating novel 2D materials, such as porous organic frameworks (COFs, MOFs, HOFs, etc.) and MXenes, into the modification of biochar. Incorporating green synthesis approaches can also enhance the integration of biochar-based materials into sensors, opening new research avenues in this field.

## Conflicts of interest

The authors declare that they have no known competing financial interests or personal relationships that could have appeared to influence the work reported in this paper.

## Data availability

The data supporting the findings of this study are available from the corresponding author upon reasonable request.

## Acknowledgements

This research did not receive any specific grant from funding agencies in the public, commercial, or not-for-profit sectors. SKK greatly acknowledges the Director SVNIT Surat for providing necessary facilities.

## References

- 1 L. Li, *et al.*, Global Greenhouse Gas Emissions From Agriculture: Pathways to Sustainable Reductions, *Global Change Biol.*, 2025, **31**(1), e70015.
- 2 T. Scandola, *et al.*, Insights into the effects of elevated atmospheric carbon dioxide on plant-virus interactions: a literature review, *Environ. Exp. Bot.*, 2024, 105737.
- 3 T. Ghanbari, F. Abnisa and W. M. A. W. Daud, A review on production of metal organic frameworks (MOF) for CO<sub>2</sub> adsorption, *Sci. Total Environ.*, 2020, **707**, 135090.
- 4 Q. A. Nwabueze and S. Leggett, Advancements in the application of CO<sub>2</sub> capture and utilization technologies—A comprehensive review, *Fuels*, 2024, **5**(3), 508–532.
- 5 F. Raganati and P. Ammendola, CO<sub>2</sub> post-combustion capture: a critical review of Current technologies and future directions, *Energy Fuels*, 2024, **38**(15), 13858–13905.
- 6 A. Zaker, *et al.*, Carbon-based materials for CO<sub>2</sub> capture: Their production, modification and performance, *J. Environ. Chem. Eng.*, 2023, **11**(3), 109741.
- 7 N. Hsan, *et al.*, Advancements in Carbon-Based Materials for Enhanced Carbon Dioxide Capture and Conversion: A Comprehensive Review, *Fibers Polym.*, 2025, 1–28.
- 8 R. Ahmed, *et al.*, Recent advances in carbon-based renewable adsorbent for selective carbon dioxide capture and separation-A review, *J. Cleaner Prod.*, 2020, **242**, 118409.
- 9 A. N. Shafawi, *et al.*, Recent advances in developing engineered biochar for CO<sub>2</sub> capture: An insight into the biochar modification approaches, *J. Environ. Chem. Eng.*, 2021, **9**(6), 106869.
- 10 K. N. Shoudho, *et al.*, Biochar in global carbon cycle: Towards sustainable development goals, *Curr. Res. Green Sustainable Chem.*, 2024, 100409.
- 11 E. Miliotti, *et al.*, Lab-scale pyrolysis and hydrothermal carbonization of biomass digestate: Characterization of solid products and compliance with biochar standards, *Biomass Bioenergy*, 2020, **139**, 105593.
- 12 N. Gao, *et al.*, Chitosan-modified biochar: Preparation, modifications, mechanisms and applications, *Int. J. Biol. Macromol.*, 2022, **209**, 31–49.
- 13 K. Li, *et al.*, Renewable biochar derived from mixed sewage sludge and pine sawdust for carbon dioxide capture, *Environ. Pollut.*, 2022, **306**, 119399.
- 14 A. Kumar, *et al.*, A green approach towards sorption of CO<sub>2</sub> on waste derived biochar, *Environ. Res.*, 2022, **214**, 113954.
- 15 X. Xu, *et al.*, Chemical transformation of CO<sub>2</sub> during its capture by waste biomass derived biochars, *Environ. Pollut.*, 2016, **213**, 533–540.
- 16 P. D. Dissanayake, *et al.*, Biochar-based adsorbents for carbon dioxide capture: A critical review, *Renewable Sustainable Energy Rev.*, 2020, **119**, 109582.
- 17 G. Ravindiran, *et al.*, Production and modifications of biochar to engineered materials and its application for environmental sustainability: A review, *Biochar*, 2024, **6**(1), 62.
- 18 Y. Tao, *et al.*, Utilization of cotton byproduct-derived biochar: a review on soil remediation and carbon sequestration, *Environ. Sci. Eur.*, 2024, **36**(1), 79.
- 19 L. Pang, *et al.*, How does natural resource depletion affect energy security risk? New insights from major energy-consuming countries, *Energy Strat. Rev.*, 2024, **54**, 101460.
- 20 Z. Jia, *et al.*, Relationship between natural resources, economic growth, and carbon emissions: the role of fintech, information technology and corruption to achieve the targets of COP-27, *Resour. Policy*, 2024, **90**, 104751.
- 21 Y. Li, *et al.*, Solid waste of calcium lignin replaces fossil fuel power by gasification to reduce CO<sub>2</sub> emissions, *Process Saf. Environ. Prot.*, 2024, **182**, 857–865.
- 22 K. O. Yoro, *et al.*, A review on heat and mass integration techniques for energy and material minimization during CO<sub>2</sub> capture, *Int. J. Energy Environ. Eng.*, 2019, **10**, 367–387.
- 23 C. Cuni-Lopez, *et al.*, Impact of wildfire smoke and diesel exhaust on inflammatory response in aging human microglia, *bioRxiv*, 2024, 629570.
- 24 S. Niture, *et al.*, Ethyltoluenes Regulate Inflammatory and Cell Fibrosis Signaling in the Liver Cell Model, *Toxics*, 2024, **12**(12), 856.



- 25 D. Schneberger, *et al.*, Effect of low-level CO<sub>2</sub> on innate inflammatory protein response to organic dust from swine confinement barns, *J. Occup. Med. Toxicol.*, 2017, **12**, 1–9.
- 26 D. Moodley, *An Evaluation of Sick Building Syndrome Amongst Administrative Employees in an Office Environment in Durban, KwaZulu-Natal*. 2021.
- 27 T. A. Jacobson, *et al.*, Direct human health risks of increased atmospheric carbon dioxide, *Nat Sustainability*, 2019, **2**(8), 691–701.
- 28 B. Diaz, *et al.*, Synthesis methods, properties, and modifications of biochar-based materials for wastewater treatment: a review, *Resources*, 2024, **13**(1), 8.
- 29 S. K. Awasthi, *et al.*, Multi-criteria research lines on livestock manure biorefinery development towards a circular economy: from the perspective of a life cycle assessment and business models strategies, *J. Cleaner Prod.*, 2022, **341**, 130862.
- 30 J. Liu, *et al.*, Biomass pyrolysis mechanism for carbon-based high-value products, *Proc. Combust. Inst.*, 2023, **39**(3), 3157–3181.
- 31 K. Yogalakshmi, *et al.*, Lignocellulosic biomass-based pyrolysis: A comprehensive review, *Chemosphere*, 2022, **286**, 131824.
- 32 S. Al Arni, Thermal Conversion of Solid Waste via Pyrolysis to Produce Bio-Oil, Biochar and Syngas, in *Advanced Technologies for Solid, Liquid, and Gas Waste Treatment*, CRC Press, 2023, pp. 41–55.
- 33 Y. Aoulad El Hadj Ali, *et al.*, Recent advances and prospects of biochar-based adsorbents for malachite green removal: a comprehensive review, *Chem. Afr.*, 2023, **6**(2), 579–608.
- 34 B. Babinszki, *et al.*, Effect of slow pyrolysis conditions on biocarbon yield and properties: Characterization of the volatiles, *Bioresour. Technol.*, 2021, **338**, 125567.
- 35 J.-S. Lu, *et al.*, Slow pyrolysis of municipal solid waste (MSW): A review, *Bioresour. Technol.*, 2020, **312**, 123615.
- 36 G. Sawargaonkar, *et al.*, Valorization of peanut shells through biochar production using slow and fast pyrolysis and its detailed physicochemical characterization, *Front. Sustain.*, 2024, **5**, 1417207.
- 37 K. K. B. S. Babu, *et al.*, Production of biochar from waste biomass using slow pyrolysis: Studies of the effect of pyrolysis temperature and holding time on biochar yield and properties, *Mater. Sci. Energy Technol.*, 2024, **7**, 318–334.
- 38 P. Premchand, *et al.*, Enhancing biochar production: A technical analysis of the combined influence of chemical activation (KOH and NaOH) and pyrolysis atmospheres (N<sub>2</sub>/CO<sub>2</sub>) on yields and properties of rice husk-derived biochar, *J. Environ. Manage.*, 2024, **370**, 123034.
- 39 D. G. Gizaw, *et al.*, Advances in solid biofuels production through torrefaction: Potential biomass, types of torrefaction and reactors, influencing process parameters and future opportunities—A review, *Process Saf. Environ. Prot.*, 2024, **186**, 1307–1319.
- 40 Y. Shen, Biomass pretreatment for steam gasification toward H<sub>2</sub>-rich syngas production—An overview, *Int. J. Hydrogen Energy*, 2024, **66**, 90–102.
- 41 A. Anu, *et al.*, Biological pretreatment of lignocellulosic biomass: An environment-benign and sustainable approach for conversion of solid waste into value-added products, *Crit. Rev. Environ. Sci. Technol.*, 2024, **54**(10), 771–796.
- 42 A. Lampropoulos, *et al.*, Effect of Olive Kernel thermal treatment (torrefaction vs. slow pyrolysis) on the physicochemical characteristics and the CO<sub>2</sub> or H<sub>2</sub>O gasification performance of as-prepared biochars, *Int. J. Hydrogen Energy*, 2021, **46**(57), 29126–29141.
- 43 D. Gogoi, *et al.*, Effect of torrefaction on yield and quality of pyrolytic products of arecanut husk: An agro-processing wastes, *Bioresour. Technol.*, 2017, **242**, 36–44.
- 44 A. Mukherjee, *et al.*, Experimental and modeling studies of torrefaction of spent coffee grounds and coffee husk: effects on surface chemistry and carbon dioxide capture performance, *ACS Omega*, 2021, **7**(1), 638–653.
- 45 Y. Sun, *et al.*, Gas-pressurized torrefaction of biomass wastes: Self-promoted deoxygenation of rice straw at low temperature, *Fuel*, 2022, **308**, 122029.
- 46 X. Gao, *et al.*, Pyrolysis of torrefied rice straw from gas-pressurized and oxidative torrefaction: pyrolysis kinetic analysis and the properties of biochars, *J. Anal. Appl. Pyrolysis*, 2021, **157**, 105238.
- 47 J. Hang, *et al.*, A super magnetic porous biochar manufactured by potassium ferrate-accelerated hydrothermal carbonization for removal of tetracycline, *J. Cleaner Prod.*, 2024, **435**, 140470.
- 48 W.-H. Chen, *et al.*, Achieving carbon credits through biomass torrefaction and hydrothermal carbonization: A review, *Renewable Sustainable Energy Rev.*, 2025, **208**, 115056.
- 49 S. Zhang, *et al.*, Pyrolytic and hydrothermal carbonization affect the transformation of phosphorus fractions in the biochar and hydrochar derived from organic materials: A meta-analysis study, *Sci. Total Environ.*, 2024, **906**, 167418.
- 50 T. Sharma, *et al.*, Parametric influence of process conditions on thermochemical techniques for biochar production: A state-of-the-art review, *J. Energy Inst.*, 2024, **113**, 101559.
- 51 S. Ye, *et al.*, Optimization of microalgal hydrothermal carbonization parameters using the response surface method for biochar applications in blast furnaces to reduce carbon emissions, *Fuel*, 2025, **381**, 133671.
- 52 R. Li and A. Shahbazi, A review of hydrothermal carbonization of carbohydrates for carbon spheres preparation, *Trends Renew. Energy*, 2015, **1**(1), 43–56.
- 53 G. Prasannamedha, *et al.*, Enhanced adsorptive removal of sulfamethoxazole from water using biochar derived from hydrothermal carbonization of sugarcane bagasse, *J. Hazard. Mater.*, 2021, **407**, 124825.
- 54 T. Zhang, *et al.*, Co-removal of CO<sub>2</sub> and Hg using corn straw and pine biochar pretreated by hydrothermal technology, *Sep. Purif. Technol.*, 2024, **342**, 127065.



- 55 T. Zhang, *et al.*, Comparative study on the adsorption performance of CO<sub>2</sub> and Hg in flue gas using corn straw and pine biochar modified by KOH, *Sep. Purif. Technol.*, 2025, **359**, 130757.
- 56 C. Liu, *et al.*, Ultramicropore-rich N-doped porous biochar from discarded cigarette butts for efficient CO<sub>2</sub> capture with ultra-high adsorption capacity and selectivity, *Sep. Purif. Technol.*, 2025, **358**, 130205.
- 57 K. Velusamy, *et al.*, Role of biochar as a greener catalyst in biofuel production: production, activation, and potential utilization—A review, *J. Taiwan Inst. Chem. Eng.*, 2024, 105732.
- 58 S. Ascher, I. Watson and S. You, Machine learning methods for modelling the gasification and pyrolysis of biomass and waste, *Renewable Sustainable Energy Rev.*, 2022, **155**, 111902.
- 59 A. Kumar and T. Bhattacharya, Biochar: a sustainable solution, *Environ. Dev. Sustain.*, 2021, **23**, 6642–6680.
- 60 L. Xiang, *et al.*, Potential hazards of biochar: The negative environmental impacts of biochar applications, *J. Hazard. Mater.*, 2021, **420**, 126611.
- 61 J. O. Ighalo, D. V. Onifade and A. G. Adeniyi, Retort-heating carbonisation of almond (*Terminalia catappa*) leaves and LDPE waste for biochar production: evaluation of product quality, *Int. J. Sustain. Eng.*, 2021, **14**(5), 1059–1067.
- 62 H. N. Nguyen, Solid residues after gasification of agricultural residues as scalable and economical CO<sub>2</sub> adsorption materials, *Adv. Bamboo Sci.*, 2024, **8**, 100105.
- 63 P. D. Dissanayake, *et al.*, Sustainable gasification biochar as a high efficiency adsorbent for CO<sub>2</sub> capture: A facile method to designer biochar fabrication, *Renewable Sustainable Energy Rev.*, 2020, **124**, 109785.
- 64 R. Potnuri, *et al.*, A review on analysis of biochar produced from microwave-assisted pyrolysis of agricultural waste biomass, *J. Anal. Appl. Pyrolysis*, 2023, **173**, 106094.
- 65 R. K. Nekouei, *et al.*, Microwave-assisted transforming of biosolids into engineered activated carbon employed for adsorption from wastewater, *J. Cleaner Prod.*, 2024, **467**, 142941.
- 66 D. V. Suriapparao, H. K. Tanneru and B. R. Reddy, A review on the role of susceptors in the recovery of valuable renewable carbon products from microwave-assisted pyrolysis of lignocellulosic and algal biomasses: Prospects and challenges, *Environ. Res.*, 2022, **215**, 114378.
- 67 Z. Li, *et al.*, Advanced mechanisms and applications of microwave-assisted synthesis of carbon-based materials: a brief review, *Nanoscale Adv.*, 2025, **7**, 419–432.
- 68 Y.-F. Huang, *et al.*, Microwave pyrolysis of rice straw to produce biochar as an adsorbent for CO<sub>2</sub> capture, *Energy*, 2015, **84**, 75–82.
- 69 Y.-F. Huang, P.-T. Chiueh and S.-L. Lo, Carbon capture of biochar produced by microwave co-pyrolysis: adsorption capacity, kinetics, and benefits, *Environ. Sci. Pollut. Res.*, 2023, **30**(9), 22211–22221.
- 70 J. Chen, *et al.*, Enhanced CO<sub>2</sub> capture performance of N, S co-doped biochar prepared by microwave pyrolysis: Synergistic modulation of microporous structure and functional groups, *Fuel*, 2025, **379**, 132987.
- 71 X. Zhang, *et al.*, Lignin-impregnated biochar assisted with microwave irradiation for CO<sub>2</sub> capture: adsorption performance and mechanism, *Biochar*, 2024, **6**(1), 22.
- 72 P. Premchand, *et al.*, Biochar production from slow pyrolysis of biomass under CO<sub>2</sub> atmosphere: A review on the effect of CO<sub>2</sub> medium on biochar production, characterisation, and environmental applications, *J. Environ. Chem. Eng.*, 2023, **11**(3), 110009.
- 73 X. Yuan, *et al.*, Active Learning-Based Guided Synthesis of Engineered Biochar for CO<sub>2</sub> Capture, *Environ. Sci. Technol.*, 2024, **58**(15), 6628–6636.
- 74 M. Ghorbani, *et al.*, How do different feedstocks and pyrolysis conditions effectively change biochar modification scenarios? A critical analysis of engineered biochars under H<sub>2</sub>O<sub>2</sub> oxidation, *Energy Convers. Manage.*, 2024, **300**, 117924.
- 75 Y. Yang, *et al.*, Effect of electric field and humic acid on the mobility of biochar particles in soil, *Environ. Technol. Innov.*, 2024, 103704.
- 76 F. C. Asif, *3D Graphene-like Carbon Structure Evolution via Microwave Pyrolysis of Hemp Biomass: A Feedstock-Process-Structure-Property Relationship Study*, 2024.
- 77 B. Behera, P. Behera and N. Sethi, Decoupling the role of renewable energy, green finance and political stability in achieving the sustainable development goal 13: Empirical insight from emerging economies, *Sustainable Dev.*, 2024, **32**(1), 119–137.
- 78 L. Cai, *et al.*, High-performance oxygen transport membrane reactors integrated with IGCC for carbon capture, *AIChE J.*, 2020, **66**(7), e16427.
- 79 P. Madejski, *et al.*, Methods and techniques for CO<sub>2</sub> capture: Review of potential solutions and applications in modern energy technologies, *Energies*, 2022, **15**(3), 887.
- 80 F. Güleç and J. A. Okolie, Decarbonising bioenergy through biomass utilisation in chemical looping combustion and gasification: a review, *Environ. Chem. Lett.*, 2024, **22**(1), 121–147.
- 81 Y. Tan, *et al.*, Conventional and optimized testing facilities of calcium looping process for CO<sub>2</sub> capture: A systematic review, *Fuel*, 2024, **358**, 130337.
- 82 J. Du, *et al.*, Review on post-combustion CO<sub>2</sub> capture by amine blended solvents and aqueous ammonia, *Chem.-Eng. J.*, 2024, 150954.
- 83 Y. Wang, *et al.*, Corrosion performance of carbon/stainless steel in amine-based solvents under different conditions for CO<sub>2</sub> chemical absorption process, *Greenhouse Gases:Sci. Technol.*, 2024, **14**, 26–41.
- 84 T. He, *et al.*, Integrated ethane recovery and cryogenic carbon capture in a dual mixed refrigerant natural gas liquefaction process, *Energy*, 2024, **290**, 130125.
- 85 X. Y. D. Soo, *et al.*, Advancements in CO<sub>2</sub> capture by absorption and adsorption: A comprehensive review, *J. CO<sub>2</sub> Util.*, 2024, **81**, 102727.
- 86 W. Wang, *et al.*, Tuning Catalytic Activity of CO<sub>2</sub> Hydrogenation to C1 Product via Metal Support Interaction Over Metal/Metal Oxide Supported Catalysts, *ChemSusChem*, 2024, e202400104.



- 87 K. Zhang and R. Wang, A critical review on new and efficient adsorbents for CO<sub>2</sub> capture, *Chem.-Eng. J.*, 2024, 149495.
- 88 S. Li, *et al.*, A review on biomass-derived CO<sub>2</sub> adsorption capture: adsorbent, adsorber, adsorption, and advice, *Renewable Sustainable Energy Rev.*, 2021, 152, 111708.
- 89 S. Yu, *et al.*, Towards negative emissions: Hydrothermal carbonization of biomass for sustainable carbon materials, *Adv. Mater.*, 2024, 2307412.
- 90 Y. X. Seow, *et al.*, A review on biochar production from different biomass wastes by recent carbonization technologies and its sustainable applications, *J. Environ. Chem. Eng.*, 2022, 10(1), 107017.
- 91 L. Zhao, *et al.*, Sewage sludge derived biochar for environmental improvement: Advances, challenges, and solutions, *Water Res.*, 2023, 18, 100167.
- 92 X. Zhang, *et al.*, Preparation and evaluation of fine-tuned micropore biochar by lignin impregnation for CO<sub>2</sub> and VOCs adsorption, *Sep. Purif. Technol.*, 2022, 295, 121295.
- 93 L. Guo, *et al.*, Role of hydrogen peroxide preoxidizing on CO<sub>2</sub> adsorption of nitrogen-doped carbons produced from coconut shell, *ACS Sustain. Chem. Eng.*, 2016, 4(5), 2806–2813.
- 94 H. Bamdad, *et al.*, Application of biochar for acid gas removal: experimental and statistical analysis using CO<sub>2</sub>, *Environ. Sci. Pollut. Res.*, 2019, 26(11), 10902–10915.
- 95 Z. G. Mamaghani, *et al.*, Wood biochar as a point source CO<sub>2</sub> adsorbent-impact of humidity on performance, *Fuel*, 2024, 361, 130737.
- 96 I. B. Salem, *et al.*, Utilization of the UAE date palm leaf biochar in carbon dioxide capture and sequestration processes, *J. Environ. Manage.*, 2021, 299, 113644.
- 97 G. Durán-Jiménez, *et al.*, Green and simple approach for low-cost bioproducts preparation and CO<sub>2</sub> capture, *Chemosphere*, 2021, 279, 130512.
- 98 A. Mukherjee, *et al.*, Carbon dioxide capture from flue gas in biochar produced from spent coffee grounds: Effect of surface chemistry and porous structure, *J. Environ. Chem. Eng.*, 2021, 9(5), 106049.
- 99 T. Taher, *et al.*, Facile synthesis of biochar/layered double oxides composite by one-step calcination for enhanced carbon dioxide (CO<sub>2</sub>) adsorption, *Mater. Lett.*, 2023, 338, 134068.
- 100 Lourenço, M.A., *et al.*, N-doped sponge-like biochar: A promising CO<sub>2</sub> sorbent for CO<sub>2</sub>/CH<sub>4</sub> and CO<sub>2</sub>/N<sub>2</sub> gas separation, *Chem. Eng. J.*, 2023, 470, 144005.
- 101 C. Liu, *et al.*, CO<sub>2</sub> capture performance of biochar prepared from sewage sludge after conditioning with different dewatering agents, *J. Environ. Chem. Eng.*, 2022, 10(5), 108318.
- 102 Y.-F. Huang, P.-T. Chiueh and S.-L. Lo, CO<sub>2</sub> adsorption on biochar from co-torrefaction of sewage sludge and leucaena wood using microwave heating, *Energy Procedia*, 2019, 158, 4435–4440.
- 103 P. Godlewska, *et al.*, Adsorption capacity of phenanthrene and pyrene to engineered carbon-based adsorbents produced from sewage sludge or sewage sludge-biomass mixture in various gaseous conditions, *Bioresour. Technol.*, 2019, 280, 421–429.
- 104 M. Kończak, *et al.*, Carbon dioxide as a carrier gas and mixed feedstock pyrolysis decreased toxicity of sewage sludge biochar, *Sci. Total Environ.*, 2020, 723, 137796.
- 105 Z. G. Mamaghani, *et al.*, Impact evaluation of coexisting gas CO on CO<sub>2</sub> adsorption on biochar derived from softwood shavings, *Sep. Purif. Technol.*, 2024, 126529.
- 106 J. Chen, *et al.*, A complete review on the oxygen-containing functional groups of biochar: Formation mechanisms, detection methods, engineering, and applications, *Sci. Total Environ.*, 2024, 174081.
- 107 A. K. Dalai and R. Azargohar, *Production of Activated Carbon from Biochar Using Chemical and Physical Activation: Mechanism and Modeling*, ACS Publications, 2007.
- 108 M. Koltowski, *et al.*, Effect of biochar activation by different methods on toxicity of soil contaminated by industrial activity, *Ecotoxicol. Environ. Saf.*, 2017, 136, 119–125.
- 109 N. A. Rashidi and S. Yusup, Biochar as potential precursors for activated carbon production: parametric analysis and multi-response optimization, *Environ. Sci. Pollut. Res.*, 2020, 27(22), 27480–27490.
- 110 A. D. Igalavithana, *et al.*, Carbon dioxide capture in biochar produced from pine sawdust and paper mill sludge: Effect of porous structure and surface chemistry, *Sci. Total Environ.*, 2020, 739, 139845.
- 111 V. Gargiulo, *et al.*, Assessing the potential of biochars prepared by steam-assisted slow pyrolysis for CO<sub>2</sub> adsorption and separation, *Energy Fuels*, 2018, 32(10), 10218–10227.
- 112 A. E. Ogungbenro, *et al.*, Physical synthesis and characterization of activated carbon from date seeds for CO<sub>2</sub> capture, *J. Environ. Chem. Eng.*, 2018, 6(4), 4245–4252.
- 113 J. J. Manyà, D. García-Morcate and B. González, Adsorption performance of physically activated biochars for postcombustion CO<sub>2</sub> capture from dry and humid flue gas, *Appl. Sci.*, 2020, 10(1), 376.
- 114 Z. Pan, *et al.*, Lignin-based hierarchical porous biochar prepared from negative pressure pyrolysis enhanced CO<sub>2</sub> and VOCs adsorption, *Sep. Purif. Technol.*, 2024, 345, 127398.
- 115 Y. Jie, *et al.*, *Efficient CO<sub>2</sub> Capture by Porous Carbons Derived from Coconut Shell*, 2017.
- 116 S. Ding and Y. Liu, Adsorption of CO<sub>2</sub> from flue gas by novel seaweed-based KOH-activated porous biochars, *Fuel*, 2020, 260, 116382.
- 117 Y. Ji, *et al.*, A high adsorption capacity bamboo biochar for CO<sub>2</sub> capture for low temperature heat utilization, *Sep. Purif. Technol.*, 2022, 293, 121131.
- 118 C. Zhang, *et al.*, Direct air capture of CO<sub>2</sub> by KOH-activated bamboo biochar, *J. Energy Inst.*, 2022, 105, 399–405.
- 119 K. Li, *et al.*, Insights into CO<sub>2</sub> adsorption on KOH-activated biochars derived from the mixed sewage sludge and pine sawdust, *Sci. Total Environ.*, 2022, 826, 154133.
- 120 C. H. Pimentel, *et al.*, Separation of CO<sub>2</sub> using biochar and KOH and ZnCl<sub>2</sub> activated carbons derived from pine sawdust, *J. Environ. Chem. Eng.*, 2023, 11(6), 111378.



- 121 C. Lim, *et al.*, Unique CO<sub>2</sub> adsorption of pine needle biochar-based activated carbons by induction of functionality transition, *J. Ind. Eng. Chem.*, 2023, **124**, 201–210.
- 122 J. Sreńscek-Nazzal, *et al.*, Chemical activation of banana peel waste-derived biochar using KOH and urea for CO<sub>2</sub> capture, *Materials*, 2024, **17**(4), 872.
- 123 A. D. Igalavithana, *et al.*, Gasification biochar from biowaste (food waste and wood waste) for effective CO<sub>2</sub> adsorption, *J. Hazard. Mater.*, 2020, **391**, 121147.
- 124 J. J. Manyà, *et al.*, Ultra-microporous adsorbents prepared from vine shoots-derived biochar with high CO<sub>2</sub> uptake and CO<sub>2</sub>/N<sub>2</sub> selectivity, *Chem. Eng. J.*, 2018, **345**, 631–639.
- 125 Y. Qiao, *et al.*, One-pot synthesis of digestate-derived biochar for carbon dioxide capture, *Fuel*, 2020, **279**, 118525.
- 126 X. Yuan, *et al.*, N, P Co-doped porous biochar derived from cornstalk for high performance CO<sub>2</sub> adsorption and electrochemical energy storage, *Sep. Purif. Technol.*, 2022, **299**, 121719.
- 127 W. Wu, *et al.*, Synergistic effects of heteroatom doping and narrow micropores on carbon dioxide capture in bamboo shoot shell-based porous carbon, *Sep. Purif. Technol.*, 2024, **339**, 126690.
- 128 J. Luo, *et al.*, Microwave-induced preparation of MgO-loaded N-rich porous biochar from marine biomass for efficient CO<sub>2</sub> capture and mechanism exploration *via* theoretical calculation, *J. Cleaner Prod.*, 2023, **405**, 136915.
- 129 B. Ji, *et al.*, Amino-modified biochar-silica hybrid aerogels with ordered pore structure templated by cellulose nanocrystals for highly efficient and selective CO<sub>2</sub> capture, *J. Cleaner Prod.*, 2024, **435**, 140501.
- 130 T. Guo, *et al.*, Surface oxidation modification of nitrogen doping biochar for enhancing CO<sub>2</sub> adsorption, *Ind. Crops Prod.*, 2023, **206**, 117582.
- 131 X. Xu, *et al.*, N-doped biochar synthesized by a facile ball-milling method for enhanced sorption of CO<sub>2</sub> and reactive red, *Chem. Eng. J.*, 2019, **368**, 564–572.
- 132 P. Lahijani, M. Mohammadi and A. R. Mohamed, Metal incorporated biochar as a potential adsorbent for high capacity CO<sub>2</sub> capture at ambient condition, *J. CO<sub>2</sub> Util.*, 2018, **26**, 281–293.
- 133 X. Xu, *et al.*, New insights into CO<sub>2</sub> sorption on biochar/Fe oxyhydroxide composites: Kinetics, mechanisms, and *in situ* characterization, *Chem. Eng. J.*, 2020, **384**, 123289.
- 134 N. A. Zubbri, *et al.*, Enhancement of CO<sub>2</sub> adsorption on biochar sorbent modified by metal incorporation, *Environ. Sci. Pollut. Res.*, 2020, **27**(11), 11809–11829.
- 135 S.-H. Liu and Y.-Y. Huang, Valorization of coffee grounds to biochar-derived adsorbents for CO<sub>2</sub> adsorption, *J. Cleaner Prod.*, 2018, **175**, 354–360.
- 136 C. Wang, *et al.*, Study on the decarbonization mechanism of composite adsorbent by Mg-MOF-74-based modified biochar, *Fuel*, 2024, **357**, 129959.
- 137 J. Zhang, *et al.*, Activation-free synthesis of nitrogen-doped biochar for enhanced adsorption of CO<sub>2</sub>, *J. Cleaner Prod.*, 2022, **355**, 131642.
- 138 L. Anson-Bertina, *et al.*, Metal–Organic Frameworks (MOFs) containing adsorbents for carbon capture, *Energies*, 2022, **15**(9), 3473.
- 139 J. Zhang, *et al.*, Broccoli-shaped Cu-BTC/biochar composite with enhanced water stability for toluene adsorption: influence of humid air aging, *Fuel*, 2023, **335**, 127013.
- 140 H. N. Nguyen, *et al.*, Investigation on cost-effective composites for CO<sub>2</sub> adsorption from post-gasification residue and metal organic framework, *J. Environ. Sci.*, 2025, **148**, 174–187.
- 141 N. T. Mai, *et al.*, Towards cost-effective CO<sub>2</sub> adsorption materials: Case of CuBTC-Hydrochar composite, *Mater. Today Commun.*, 2024, **38**, 107619.
- 142 N. M. Amer, *et al.*, Woody Biomass-Derived Biochar Decorated with Vanadium Oxide as a Potential Adsorbent for CO<sub>2</sub> Capture, *Int. J. Environ. Res.*, 2024, **18**(3), 43.
- 143 A. E. Creamer, *et al.*, Biomass-facilitated production of activated magnesium oxide nanoparticles with extraordinary CO<sub>2</sub> capture capacity, *Chem. Eng. J.*, 2018, **334**, 81–88.
- 144 R. Venkatesh, *et al.*, Synthesis and adsorbent performance of modified biochar with Ag/MgO nanocomposites for heat storage application, *Adsorpt. Sci. Technol.*, 2022, **2022**, 7423102.
- 145 W. Cao, *et al.*, Novel post-treatment of ultrasound assisting with acid washing enhance lignin-based biochar for CO<sub>2</sub> capture: adsorption performance and mechanism, *Chem. Eng. J.*, 2023, **471**, 144523.
- 146 M. Li and R. Xiao, Preparation of a dual pore structure activated carbon from rice husk char as an adsorbent for CO<sub>2</sub> capture, *Fuel Process. Technol.*, 2019, **186**, 35–39.
- 147 Y. Zhou, *et al.*, Adsorption of CO<sub>2</sub> by nitrogen doped corn straw based biochar, *Arabian J. Geosci.*, 2021, **14**(18), 1875.
- 148 F. D. Prochnow, *et al.*, Biochar: from laboratory to industry scale—an overview of scientific and industrial advances, opportunities in the Brazilian context, and contributions to sustainable development, *Processes*, 2024, **12**(5), 1006.
- 149 T. Terzić, *et al.*, A Review on Ionic Liquids in the Design of Carbon-Based Materials for Environmental Contaminant Removal, *Processes*, 2026, **14**(2), 352.
- 150 J. F. Saldarriaga and J. E. López, Biochar as a Bridge Between Biomass Energy Technologies and Sustainable Agriculture: Opportunities, Challenges, and Future Directions, *Sustainability*, 2025, **17**(24), 11285.
- 151 H. Kua and S. Tan, Novel typology of accelerated carbonation curing: using dry and pre-soaked biochar to tune carbon capture and mechanical properties of cementitious mortar, *Biochar*, 2023, **5**(1), 36.
- 152 Y. Chen, *et al.*, Accelerated carbonation curing of biochar-cement mortar: Effects of biochar pyrolysis temperatures on carbon sequestration, mechanical properties and microstructure, *Constr. Build. Mater.*, 2024, **449**, 138446.
- 153 H. Kua, A. Goel and J. Teo, Carbon mineralization, microstructure development and mechanical properties of limestone calcined clay cement enhanced with rice husk ash and biochar (bio-LC3), *J. Cleaner Prod.*, 2025, **520**, 146091.



- 154 Z. G. Mamaghani, *et al.*, Impact evaluation of coexisting gas CO on CO<sub>2</sub> adsorption on biochar derived from softwood shavings, *Sep. Purif. Technol.*, 2024, **338**, 126529.
- 155 Z. Tang, *et al.*, Ultra-microporous biochar-based carbon adsorbents by a facile chemical activation strategy for high-performance CO<sub>2</sub> adsorption, *Fuel Process. Technol.*, 2023, **241**, 107613.
- 156 Z. Yildiz, *et al.*, Pyrolysis and optimization of chicken manure wastes in fluidized bed reactor: CO<sub>2</sub> capture in activated bio-chars, *Process Saf. Environ. Prot.*, 2019, **130**, 297–305.
- 157 R. Chatterjee, *et al.*, Effect of pyrolysis temperature on physicochemical properties and acoustic-based amination of biochar for efficient CO<sub>2</sub> adsorption, *Front. Energy Res.*, 2020, **8**, 85.
- 158 R. Chatterjee, *et al.*, Impact of biomass sources on acoustic-based chemical functionalization of biochars for improved CO<sub>2</sub> adsorption, *Energy Fuels*, 2020, **34**(7), 8608–8627.
- 159 S. Shi, *et al.*, Porous biochars derived from microalgae pyrolysis for CO<sub>2</sub> adsorption, *Energy Fuels*, 2021, **35**(9), 7646–7656.
- 160 H. Li, *et al.*, Molecular simulation combined with DFT calculation guided heteroatom-doped biochar rational design for highly selective and efficient CO<sub>2</sub> capture, *Chem. Eng. J.*, 2024, **481**, 148362.
- 161 C. Liu, *et al.*, CO<sub>2</sub> capture using biochar derived from conditioned sludge via pyrolysis, *Sep. Purif. Technol.*, 2023, **314**, 123624.
- 162 H. Bamdad, K. Hawboldt and S. MacQuarrie, Nitrogen functionalized biochar as a renewable adsorbent for efficient CO<sub>2</sub> removal, *Energy Fuels*, 2018, **32**(11), 11742–11748.
- 163 R. Chatterjee, *et al.*, Ultrasound cavitation intensified amine functionalization: a feasible strategy for enhancing CO<sub>2</sub> capture capacity of biochar, *Fuel*, 2018, **225**, 287–298.

